

Liquefaction Resistance Based on Shear Wave Velocity

By Ronald D. Andrus¹ and Kenneth H. Stokoe, II²

¹Research Civil Engineer
National Institute of Standards and Technology

²Professor of Civil Engineering
The University of Texas at Austin

Abstract

This report reviews the current simplified procedures for evaluating the liquefaction resistance of granular soil deposits using small-strain shear wave velocity. These procedures were developed from analytical studies, laboratory studies, or very limited field performance data. Their accuracy is evaluated through field performance data from 20 earthquakes and in situ shear wave velocity measurements at over 50 different sites (124 test arrays) in soils ranging from sandy gravel with cobbles to profiles including silty clay layers, resulting in a total of 193 liquefaction and non-liquefaction case histories. The current procedures correctly predict high liquefaction potential at many sites where surface manifestations of liquefaction were observed. Revisions and enhancements to the current procedures are proposed using the compiled case history data. The recommended procedure follows the general format of the SPT- and CPT-based procedures. Liquefaction potential boundaries are established by applying a modified relationship between shear wave velocity and cyclic stress ratio for constant average cyclic shear strain suggested by Dobry. These new boundaries, which are simply defined mathematically and easy to implement, correctly predict moderate to high liquefaction potential for more than 95% of the liquefaction case histories. Additional case histories are needed of all types of soils that have and have not liquefied during earthquakes, particularly from deeper deposits (depth > 8 m) and from denser soils ($V_S > 200$ m/s) shaken by stronger ground motions ($a_{\max} > 0.4$ g), to further validate the proposed procedures.

This report is a U.S. Government work and, as such, is in the public domain of the United States of America.

Evaluation of Liquefaction Resistance of Soils. National Center for Earthquake Engineering Research (NCEER) Workshop. Proceedings. January 5-6, 1996, Salt Lake, UT, Youd, T. L., Idriss, I. M., Editors, 89-128 pp, 1997.

Introduction

During the past decade, several simplified procedures using small-strain shear wave velocity, V_S , have been proposed for assessing the liquefaction resistance of granular soils (Stokoe et al. 1988b; Tokimatsu et al. 1991a; Robertson et al. 1992; Kayen et al. 1992; Andrus 1994; Lodge 1994). The use of V_S as an index of liquefaction resistance is justified since both V_S and liquefaction resistance are influenced by many of the same factors (e.g. void ratio, effective confining pressure, stress history, and geologic age).

The in situ V_S can be measured by a number of techniques such as the crosshole seismic test, the Seismic Cone Penetration Test (SCPT), or the Spectral-Analysis-of-Surface-Wave (SASW) test. The accuracy of these techniques can be sensitive to procedural details, soil conditions, and interpretation methods. Some advantages of using V_S are:

- Measurements are possible in soils that are hard to sample, such as gravelly soils, and at sites where borings or soundings may not be permitted, such as capped landfills;
- Measurements can be performed in small laboratory specimens, allowing direct comparisons between measured laboratory and field behavior;
- V_S is directly related to small-strain shear modulus, G_{max} , a parameter required in analytical procedures for estimating dynamic shearing strain in soils; and
- For large earthquake magnitudes and long durations of shaking, the cyclic shear strain needed for liquefaction decreases and approaches the threshold strain in sand ($\approx 0.02\%$), thus making it possible to conduct analytical evaluations of liquefaction using V_S and G_{max} as basic parameters (Dobry et al. 1981; Seed et al. 1983).

Two limitations of using V_S to evaluate liquefaction resistance are: (1) Field seismic measurements are made with small strains, whereas liquefaction is a large-strain phenomenon (Roy et al. 1996). This limitation can be significant for cemented soils, since V_S is highly sensitive to weak interparticle bonding which is eliminated at large strains. (2) Seismic testing does not provide samples for classification of soils and identification of non-liquefiable soft clay-rich soils. Non-liquefiable soils by the so-called Chinese criteria have clay contents (particles smaller than $5 \mu\text{m}$) greater than 15%, liquid limits greater than 35%, or moisture contents less than 90% of the liquid limit (Seed and Idriss 1982). To compensate for these limitations, a limited number of borings should be drilled and samples taken to identify weakly cemented soils that might be liquefiable but classed as non-liquefiable by V_S criteria and also to identify non-liquefiable clay-rich soils that otherwise might be classed as liquefiable.

The purpose of this report is to recommend guidelines for evaluating liquefaction resistance using in situ measurements of V_S . To accomplish this purpose, current procedures are reviewed and their accuracy is evaluated using V_S measurements at over 50 different sites (124 test arrays) and field performance data from 20 earthquakes, resulting in a total of 193 liquefaction and non-liquefaction case histories.

Earthquake and site characteristics used in the evaluations are summarized in Table 1. In Column 2 of Table 1, test array refers to the two boreholes used for crosshole measurements, the borehole (or cone sounding) and source used for downhole measurements, or the line of receivers used for SASW measurements. The occurrence of liquefaction is based on the appearance of sand boils, ground cracks and fissures, or ground settlement. The shear wave velocities used in the subsequent evaluations are either the average or minimum of values reported by the investigator(s) for the most vulnerable layer at the test array. Shown in Fig. 1 are the relationships between shear wave velocity and depth. Some of the velocities are from measurements made before the earthquake, and others are from measurements made following the earthquake. The values of total vertical stress, σ_v , and effective vertical stress, σ'_v , listed in Columns 8 and 9 of Table 1 are averages for the depth range of the measurements, estimated using total unit weights reported by the investigator(s). When no values are reported, total unit weights of 17.3 kN/m^3 for soils above the water table and 18.9 kN/m^3 for soils below the water table are assumed. The materials comprising the most vulnerable layer at all sites are Holocene to latest Pleistocene age ($< 15,000$ years). The peak horizontal ground surface accelerations, a_{max} , used in subsequent evaluations are either the peak value for the larger of the x and y ground motion records or the average of peak values for the x and y ground motion records that would have occurred at the site in the absence of liquefaction. Values of a_{max} are determined by averaging estimates reported by the investigator(s) and estimates made as part of this study using attenuation relationships developed from published ground surface acceleration data.

The proposed liquefaction assessment procedures can be divided into three general categories: (1) procedures developed from analytical studies; (2) procedures developed from laboratory studies; and (3) procedures developed from field performance studies.

Procedures Developed From Analytical Studies

Stokoe et al. (1988b) applied the cyclic strain approach developed by Dobry and his colleagues (1982) in a parametric study of the liquefaction potential of sandy soils in the Imperial Valley, California. In the cyclic strain approach, the peak cyclic shearing strain at which the cyclic pore water pressure equals the confining pressure is used as the criterion for liquefaction occurrence.

Two generalized soil profiles were used in the parametric study. The first generalized soil profile contained a shallow ($\leq 12 \text{ m}$) liquefiable sand layer. The three parameters of the sand layer which were varied are: soil stiffness in terms of V_S (or small-strain shear modulus), depth, and thickness. Depicted in Fig. 2a are three variations of the first generalized soil profile. The second generalized soil profile is presented in Fig. 2b, and was simply a 61-m thick clay deposit representative of a soil site in the Imperial Valley upon which strong-motion accelerographs

Table 1 - Vs-based Liquefaction and Non-liquefaction Case Histories

Site (1)	Test array (2)	Measurement type (3)	Liquefaction observed? (4)	Water table depth (m) (5)	Top of layer depth (m) (6)	Layer thickness (m) (7)	σ_v (kPa) (8)	σ'_v (kPa) (9)	Soil type (10)	Average Vs (m/s) (11)	Average Vs1 (m/s) (12)	Average a_{max} (g) (13)	Cyclic stress ratio (14)	Reference (15)
(a) 1906 San Francisco, California Earthquake ($M_w = 7.7$)														
Coyote Creek	SR1	crosshole	yes	2.4	3.5	2.5	83.6	62.1	sand & gravel	136	153	0.36	0.30	Youd and Hoose (1978); Barrow (1983); Bennett and Tinsley (1995)
	R1R2	crosshole	yes	2.4	3.5	2.5	75.4	58.2		154	177	0.36	0.29	
	R1R3	crosshole	yes	2.4	3.5	2.5	75.4	58.2		161	185	0.36	0.29	
	R2R3	crosshole	yes	2.4	3.5	2.5	75.4	58.2		173	198	0.36	0.29	
Salinas River, north	SR1	crosshole	no	6.0	9.1	1.5	178.2	140.8	sandy silt	177	162	0.32	0.24	
	R1R2	crosshole	no	6.0	9.1	1.5	178.2	140.8		195	179	0.32	0.24	
	R1R3	crosshole	no	6.0	9.1	1.5	178.2	140.8		200	184	0.32	0.24	
	R2R3	crosshole	no	6.0	9.1	1.5	178.2	140.8		199	183	0.32	0.24	
Salinas River, south	SR1	crosshole	yes	6.0	6.5	4.5	142.2	123.5	sand & silty sand	131	124	0.32	0.22	
	R1R2	crosshole	yes	6.0	6.5	4.5	142.2	123.5		149	141	0.32	0.22	
	R1R3	crosshole	yes	6.0	6.5	4.5	142.2	123.5		158	150	0.32	0.22	
	R2R3	crosshole	yes	6.0	6.5	4.5	142.2	123.5		168	159	0.32	0.22	
(b) 1964 Niigata, Japan Earthquake ($M_w = 7.5$)														
Niigata City	A1	SASW	no	5.0	5.0	2.5	110.9	97.7	sand	163	164	0.16	0.11	Tokimatsu et al. (1991a)
	C1	SASW	yes	1.2	1.6	6.5	90.0	54.7		115	136	0.16	0.16	
	C2	SASW	yes	1.2	1.2	4.8	67.8	44.5		118	148	0.16	0.14	
(c) 1975 Haiheng, PRC Earthquake ($M_w = 7.1$)														
Paper Mill		downhole	yes	1.0	3.0	2.0	54.7	35.3	clayey silt	122	158	0.12	0.12	Arulanandan et al. (1986)
Glass Fiber		downhole	yes	0.8	3.0	3.5	90.0	50.1	sandy silt to clayey silt	98	117	0.12	0.14	
Construction Building		downhole	yes	1.5	5.0	4.5	124.9	73.7	clayey silt	103	111	0.12	0.13	
Fishery & Shipbuilding		downhole	yes	0.5	2.5	4.0	81.7	43.6	silty sand to clayey silt	101	124	0.12	0.14	
Middle School		downhole	no	1.0	9.0	2.5	191.8	101.2	clayey silt	143	142	0.12	0.13	
Chemical Fiber		downhole	marginal	1.5	6.0	5.5	159.4	90.1	sand to clayey silt	147	152	0.12	0.13	
(d) 1979 Imperial Valley, California Earthquake ($M_w = 6.5$)														
Wildlife	1	crosshole	no	1.5	2.5	4.3	83.8	53.9	silty sand to sandy silt	127	148	0.13	0.13	Bennett et al. (1981, 1984); Sykora and Stokoe (1982); Youd and Bennett (1983); Bierschwale and Stokoe (1984); Stokoe and Nazarian (1984); Dobry et al. (1992)
	2	crosshole	no	1.5	2.5	4.3	83.8	53.9		124	145	0.13	0.13	
		SASW	no	1.5	2.5	4.3	91.8	57.8		115	132	0.13	0.13	
Radio Tower		SASW	yes	2.0	2.7	3.4	79.2	55.8	silty sand to sandy silt	90	104	0.21	0.18	
McKim		SASW	yes	1.4	1.4	3.5	54.3	38.1	silty sand	126	161	0.51	0.45	
Vail Canal		SASW	no	2.7	2.7	2.8	70.4	58.4	sand to silty sand	101	116	0.12	0.10	
Kornbloom		SASW	no	2.5	2.5	3.5	74.7	57.8	sandy silt	105	120	0.12	0.09	
Heber Road, channel fill	SR1	crosshole	yes	2.0	2.0	3.3	63.0	48.0	silty sand	131	158	0.50	0.41	
	R1R2	crosshole	yes	2.0	2.0	3.3	63.0	48.0		133	160	0.50	0.41	
Heber Road, point bar	SR1	crosshole	no	2.0	2.0	2.3	60.1	46.6	sand	164	200	0.50	0.40	
	R1R2	crosshole	no	2.0	2.0	2.3	60.1	46.6		173	210	0.50	0.40	

Table 1 (cont.) - Vs-based Liquefaction and Non-liquefaction Case Histories

(1)	(2)	(3)	(4)	(5)	(6)	(7)	(8)	(9)	(10)	(11)	(12)	(13)	(14)	(15)
(e) 1980 Mid-Chiba, Japan Earthquake ($M_w = 5.9$)														
Owi Island No. 1	C2, upper C2, lower	downhole downhole	no no	1.35 1.35	4.5 13.0	3.3 3.6	105.4 251.6	59.2 120.2	silty sand	155 195	178 186	0.08 0.08	0.09 0.08	Ishihara et al. (1981; 1987)
(f) 1981 Westmorland, California Earthquake ($M_w = 5.9$)														
Wildlife	1 2	crosshole crosshole SASW	yes yes yes	1.5 1.5 1.5	2.5 2.5 2.5	4.3 4.3 4.3	83.8 83.8 91.8	53.9 53.9 57.8	silty sand to sandy silt	127 124 115	148 145 132	0.27 0.27 0.27	0.26 0.26 0.27	Bennett et al. (1981; 1984); Sykora and Stokoe (1982); Youd and Bennett (1983); Bierschwale and Stokoe (1984); Stokoe and Nazarian (1984); Dobry et al. (1992)
Radio Tower		SASW	yes	2.0	2.7	3.4	79.2	55.8	silty sand to sandy silt	90	104	0.20	0.18	
McKim		SASW	no	1.4	1.4	3.5	54.3	38.1	silty sand	126	161	0.06	0.05	
Vail Canal		SASW	yes	2.7	2.7	2.8	70.4	58.4	sand to silty sand	101	116	0.30	0.23	
Kornbloom		SASW	yes	2.5	2.5	3.5	74.7	57.8	sandy silt	105	120	0.36	0.29	
Heber Road, channel fill	SR1 R1R2	crosshole crosshole	no no	2.0 2.0	2.0 2.0	3.3 3.3	63.0 63.0	48.0 48.0	silty sand	131 133	158 160	0.02 0.02	0.02 0.02	
Heber Road, point bar	SR1 R1R2	crosshole crosshole	no no	2.0 2.0	2.0 2.0	2.3 2.3	60.1 60.1	46.6 46.6	sand	164 173	200 210	0.02 0.02	0.02 0.02	
(g) 1983 Borah Peak, Idaho Earthquake ($M_w = 6.9$)														
Pence Ranch	SA1 SA2 SA3 SA4 SA5 SAA SAB SAC SAD SAE XDXE	SASW SASW SASW SASW SASW SASW SASW SASW SASW SASW crosshole	yes yes yes yes yes yes yes yes yes yes yes	1.7 1.5 1.4 1.8 1.5 2.0 1.5 1.5 1.5 1.7 1.5	1.8 1.5 1.4 1.8 1.5 2.0 1.5 1.5 1.5 1.7 1.5	1.9 2.8 1.8 2.8 1.9 1.7 1.7 1.9 1.7 1.5 2.3	57.2 52.7 44.5 62.1 60.5 57.5 38.8 38.4 39.4 43.3 48.5	46.2 40.5 36.0 49.4 45.6 46.3 32.9 32.4 33.8 38.3 38.1	gravelly sand to sandy gravel	107 94 102 109 122 134 128 107 131 122 154	131 118 132 131 151 164 170 142 173 155 198	0.36 0.36 0.36 0.36 0.36 0.36 0.36 0.36 0.36 0.36 0.36	0.28 0.29 0.28 0.28 0.29 0.28 0.26 0.27 0.26 0.26 0.29	Andrus and Youd (1987); Stokoe et al. (1988a); Andrus et al. (1992); Andrus (1994)
Goddard Ranch	SA2 SA4	SASW SASW	yes yes	1.2 1.2	1.2 1.2	2.0 2.0	47.3 41.1	36.0 32.7	sandy gravel	122 105	158 137	0.30 0.30	0.24 0.23	
Andersen Bar	X1X2 SA1	crosshole SASW	yes yes	0.8 0.8	0.8 0.8	2.4 2.4	40.6 39.0	28.7 27.8	sandy gravel	106 105	146 145	0.29 0.29	0.26 0.25	
Larter Ranch	X3X4 SA1.85 SA1.90	crosshole SASW SASW	yes yes yes	0.8 0.8 0.8	2.2 2.2 2.2	1.3 1.3 1.3	59.9 55.4 59.9	39.0 38.4 40.5	silty sandy gravel	176 153 183	223 194 230	0.50 0.50 0.50	0.49 0.46 0.47	
Whiskey Springs	WS1a SA5	crosshole SASW	yes yes	0.8 0.8	1.8 1.8	2.2 2.2	59.1 45.6	38.2 31.7	sandy silty gravel	181 210	230 271	0.50 0.50	0.49 0.46	
North Gravel Bar	SA1 SA2	SASW SASW	no no	1.0 3.0	1.8 3.0	1.2 1.3	51.0 75.2	36.0 53.5	sandy gravel	206 274	266 322	0.46 0.46	0.41 0.42	
Mackay Dam, downstream toe	SA2	SASW	no	2.3	2.3	2.7	66.6	57.4	silty sandy gravel	271	313	0.23	0.17	
(h) 1985 Chiba-Ibaragi-Kenkyo, Japan Earthquake ($M_w = 6.0$)														
Owi Island No. 1	C2, upper C2, lower	downhole downhole	no no	1.35 1.35	4.5 13.0	3.3 3.6	105.4 251.6	59.2 120.2	silty sand	155 195	178 186	0.06 0.06	0.07 0.06	Ishihara et al. (1987)
(i) 1/16/86 Taiwan Earthquake ($M_w = 6.6$; Event LSST4)														
Lotung LSST Facility	L8L3 L8L4 L2L5L6 L2L7	crosshole crosshole crosshole crosshole	no no no no	0.5 0.5 0.5 0.5	2.0 2.0 2.0 2.0	5.0 5.0 5.0 5.0	85.4 85.4 85.4 85.4	35.4 35.4 35.4 35.4	silty sand to sandy silt	146 133 127 130	190 173 166 171	0.22 0.22 0.22 0.22	0.33 0.33 0.33 0.33	Shen et al. (1991); EPRI (1992)
(j) 5/20/86 Taiwan Earthquake ($M_w = 6.6$; Event LSST7)														
Lotung LSST Facility	L8L3 L8L4 L2L5L6 L2L7	crosshole crosshole crosshole crosshole	no no no no	0.5 0.5 0.5 0.5	2.0 2.0 2.0 2.0	5.0 5.0 5.0 5.0	85.4 85.4 85.4 85.4	35.4 35.4 35.4 35.4	silty sand to sandy silt	146 133 127 130	190 173 166 171	0.18 0.18 0.18 0.18	0.27 0.27 0.27 0.27	Shen et al. (1991); EPRI (1992)

Table 1 (cont.) - Vs-based Liquefaction and Non-liquefaction Case Histories

(1)	(2)	(3)	(4)	(5)	(6)	(7)	(8)	(9)	(10)	(11)	(12)	(13)	(14)	(15)
(k) 5/20/86 Taiwan Earthquake ($M_w = 6.2$; Event LSST8)														
Lotung LSST Facility	L8L3	crosshole	no	0.5	2.0	5.0	85.4	35.4	silty sand	146	190	0.04	0.06	Shen et al. (1991); EPRI (1992)
	L8L4	crosshole	no	0.5	2.0	5.0	85.4	35.4	to sandy	133	173	0.04	0.06	
	L2L5L6	crosshole	no	0.5	2.0	5.0	85.4	35.4	silt	127	166	0.04	0.06	
	L2L7	crosshole	no	0.5	2.0	5.0	85.4	35.4		130	171	0.04	0.06	
(l) 7/30/86 Taiwan Earthquake ($M_w = 6.2$; Event LSST12)														
Lotung LSST Facility	L8L3	crosshole	no	0.5	2.0	5.0	85.4	35.4	silty sand	146	190	0.18	0.27	Shen et al. (1991); EPRI (1992)
	L8L4	crosshole	no	0.5	2.0	5.0	85.4	35.4	to sandy	133	173	0.18	0.27	
	L2L5L6	crosshole	no	0.5	2.0	5.0	85.4	35.4	silt	127	166	0.18	0.27	
	L2L7	crosshole	no	0.5	2.0	5.0	85.4	35.4		130	171	0.18	0.27	
(m) 7/30/86 Taiwan Earthquake ($M_w = 6.2$; Event LSST13)														
Lotung LSST Facility	L8L3	crosshole	no	0.5	2.0	5.0	85.4	35.4	silty sand	146	190	0.05	0.08	Shen et al. (1991); EPRI (1992)
	L8L4	crosshole	no	0.5	2.0	5.0	85.4	35.4	to sandy	133	173	0.05	0.08	
	L2L5L6	crosshole	no	0.5	2.0	5.0	85.4	35.4	silt	127	166	0.05	0.08	
	L2L7	crosshole	no	0.5	2.0	5.0	85.4	35.4		130	171	0.05	0.08	
(n) 11/4/86 Taiwan Earthquake ($M_w = 6.2$; Event LSST16)														
Lotung LSST Facility	L8L3	crosshole	no	0.5	2.0	5.0	85.4	35.4	silty sand	146	190	0.16	0.24	Shen et al. (1991); EPRI (1992)
	L8L4	crosshole	no	0.5	2.0	5.0	85.4	35.4	to sandy	133	173	0.16	0.24	
	L2L5L6	crosshole	no	0.5	2.0	5.0	85.4	35.4	silt	127	166	0.16	0.24	
	L2L7	crosshole	no	0.5	2.0	5.0	85.4	35.4		130	171	0.16	0.24	
(o) 1987 Chiba-Toho-Oki, Japan Earthquake ($M_w = 6.5$)														
Sunamachi		downhole	no	6.2	6.2	5.8	168.2	140.2	sand with silt to silty sand	150	138	0.10	0.07	Ishihara et al. (1989)
(p) 1987 Elmore Ranch, California Earthquake ($M_w = 5.9$)														
Wildlife	1	crosshole	no	1.5	2.5	4.3	83.8	53.9	silty sand	127	148	0.12	0.12	Bennett et al. (1981, 1984); Sykora and Stokoe (1982); Youd and Bennett (1983); Bierschwale and Stokoe (1984); Stokoe and Nazarian (1984); Dobry et al. (1992)
	2	crosshole	no	1.5	2.5	4.3	83.8	53.9	to sandy	124	145	0.12	0.12	
		SASW	no	1.5	2.5	4.3	91.8	57.8	silt	115	132	0.12	0.12	
Radio Tower		SASW	no	2.0	2.7	3.4	79.2	55.8	silty sand to sandy silt	90	104	0.11	0.10	
McKim		SASW	no	1.4	1.4	3.5	54.3	38.1	silty sand	126	161	0.06	0.05	
Vail Canal		SASW	no	2.7	2.7	2.8	70.4	58.4	sand to silty sand	101	116	0.13	0.10	
Kornbloom		SASW	no	2.5	2.5	3.5	74.7	57.8	sandy silt	105	120	0.24	0.19	
Heber Road, channel fill	SR1	crosshole	no	2.0	2.0	3.3	63.0	48.0	silty sand	131	158	0.03	0.02	
	R1R2	crosshole	no	2.0	2.0	3.3	63.0	48.0		133	160	0.03	0.02	
Heber Road, point bar	SR1	crosshole	no	2.0	2.0	2.3	60.1	46.6	sand	164	200	0.03	0.02	
	R1R2	crosshole	no	2.0	2.0	2.3	60.1	46.6		173	210	0.03	0.02	
(q) 1987 Superstition Hills, California Earthquake ($M_w = 6.5$)														
Wildlife	1	crosshole	yes	1.5	2.5	4.3	83.8	53.9	silty sand	127	148	0.20	0.19	Bennett et al. (1981, 1984); Sykora and Stokoe (1982); Youd and Bennett (1983); Bierschwale and Stokoe (1984); Stokoe and Nazarian (1984); Dobry et al. (1992)
	2	crosshole	yes	1.5	2.5	4.3	83.8	53.9	to sandy	124	145	0.20	0.19	
		SASW	yes	1.5	2.5	4.3	91.8	57.8	silt	115	132	0.20	0.20	
Radio Tower		SASW	no	2.0	2.7	3.4	79.2	55.8	silty sand to sandy silt	90	104	0.20	0.18	
McKim		SASW	no	1.4	1.4	3.5	54.3	38.1	silty sand	126	161	0.19	0.17	
Vail Canal		SASW	no	2.7	2.7	2.8	70.4	58.4	sand to silty sand	101	116	0.20	0.15	
Kornbloom		SASW	no	2.5	2.5	3.5	74.7	57.8	sandy silt	105	120	0.21	0.17	
Heber Road, channel fill	SR1	crosshole	no	2.0	2.0	3.3	63.0	48.0	silty sand	131	158	0.18	0.15	
	R1R2	crosshole	no	2.0	2.0	3.3	63.0	48.0		133	160	0.18	0.15	
Heber Road, point bar	SR1	crosshole	no	2.0	2.0	2.3	60.1	46.6	sand	164	200	0.18	0.15	
	R1R2	crosshole	no	2.0	2.0	2.3	60.1	46.6		173	210	0.18	0.15	

Table 1 (cont.) - Vs-based Liquefaction and Non-liquefaction Case Histories

(1)	(2)	(3)	(4)	(5)	(6)	(7)	(8)	(9)	(10)	(11)	(12)	(13)	(14)	(15)
(r) 1989 Loma Prieta, California Earthquake ($M_w = 7.0$)														
Treasure Island, fire station	X1X2 B2B3 B1B4 B4B5 B2B4	crosshole crosshole crosshole crosshole SASW downhole downhole SCPT	marginal marginal marginal marginal marginal marginal marginal marginal	1.4 1.4 1.4 1.4 1.4 1.4 1.4 1.4	4.2 4.5 4.5 4.5 4.5 4.5 4.5 4.5	7.3 7.7 7.7 7.7 7.7 7.7 7.7 7.7	106.6 148.7 147.2 101.3 118.5 139.9 163.0 154.4 146.3	63.5 83.7 83.0 60.9 69.2 78.6 90.6 86.4 82.5	silty sand to clayey silty sand	130 157 157 131 136 148 137 152 146	145 164 165 148 150 145 142 158 154	0.14 0.14 0.14 0.14 0.14 0.14 0.14 0.14 0.14	0.15 0.15 0.15 0.15 0.15 0.15 0.15 0.15 0.15	Furhriman (1993); Andrus (1994); Redpath (1991); Gibbs et al. (1992); Hryciw et al. (1991); Rollins et al. (1994)
Treasure Island, perimeter	UM03 UM05 UM06 UM09 UM11	SCPT SCPT SCPT SCPT SCPT	no yes yes yes yes	1.5 2.4 1.4 2.7 1.4	4.4 3.5 2.0 2.7 4.0	5.6 4.5 4.0 3.7 3.0	133.1 102.6 75.4 82.1 101.2	77.5 71.0 48.8 65.9 61.2	sand to silty sand	178 163 154 143 160	190 178 185 160 181	0.14 0.15 0.14 0.15 0.14	0.15 0.14 0.14 0.12 0.15	Hryciw (1991); Hryciw et al. (1991); Geomatrix (1990)
Port of Richmond	SR1 R1R2 POR2 POR3 POR4	crosshole crosshole SASW SCPT SCPT SCPT	yes yes yes yes yes yes	3.5 3.5 3.5 3.5 3.5 3.5	4.0 4.0 4.0 4.0 5.0 5.0	4.0 4.0 4.0 4.0 2.0 2.0	110.1 110.1 97.0 98.9 98.9 98.9	84.7 84.7 78.8 79.4 79.4 79.4	silt to silty sand	143 135 117 152 121 138	149 140 124 161 128 147	0.16 0.16 0.16 0.16 0.16 0.16	0.13 0.13 0.12 0.12 0.12 0.12	Stokoe et al. (1992); Mitchell et al. (1994)
Port of Richmond, Hall Ave.	SR1 R1R2	crosshole crosshole SASW	no no no	3.5 3.5 3.5	3.5 3.5 3.5	5.0 5.0 5.0	104.4 104.4 109.2	82.0 82.0 84.3	silty to silty sand	148 145 133	155 152 139	0.16 0.16 0.16	0.12 0.12 0.12	
Bay Bridge Toll Plaza	SR1 R1R2 SFOBB1 SFOBB2	crosshole crosshole SCPT SCPT	yes yes yes yes	3.0 3.0 3.0 3.0	5.5 5.5 5.5 6.0	1.5 1.5 1.5 3.0	115.9 115.9 108.3 136.6	82.4 82.4 78.8 92.4	sand to silty sand	134 134 146 148	141 141 155 151	0.24 0.24 0.24 0.24	0.21 0.21 0.21 0.22	
Port of Oakland	SR1 R1R2 POO71 POO72 POO73	crosshole crosshole SASW SCPT SCPT SCPT	yes yes yes yes yes yes	3.0 3.0 3.0 3.0 3.0 3.0	5.5 5.5 5.5 5.5 5.5 5.5	2.5 2.5 2.5 2.5 2.5 1.5	121.6 121.6 115.8 122.5 122.5 113.1	85.8 85.8 83.1 86.2 86.2 81.7	sand	145 179 157 142 145 176	151 186 165 148 150 185	0.24 0.24 0.24 0.24 0.24 0.24	0.21 0.21 0.21 0.21 0.21 0.21	
Bay Farm Island, dike	SR1 R1R2	crosshole crosshole SASW	no no no	3.6 3.6 3.6	3.6 3.6 3.6	2.8 2.8 2.8	87.1 87.1 91.9	75.2 75.2 77.0	sand	193 212 204	207 227 219	0.27 0.27 0.27	0.20 0.20 0.20	
Bay Farm Island, So. Loop Road	SR1 R1R2	crosshole crosshole SASW	yes yes yes	3.0 3.0 3.0	3.0 3.0 3.0	1.7 1.7 1.7	69.9 69.9 67.0	60.9 60.9 59.6	sand	97 116 125	109 131 143	0.27 0.27 0.27	0.20 0.20 0.19	
Marina District	school 2 3 4 5	downhole SASW SASW SASW SASW	yes yes yes yes no	2.7 2.9 2.9 2.9 5.9	2.7 2.9 2.9 2.9 5.9	1.6 7.1 7.1 2.1 4.1	61.9 117.0 117.0 69.9 140.6	54.4 82.2 82.2 59.6 105.7	sand to silty sand	153 120 105 120 220	177 129 113 137 217	0.15 0.15 0.15 0.15 0.15	0.11 0.12 0.12 0.11 0.12	Kayen et al. (1990); Tokimatsu et al. (1991b)
Coyote Creek	SR1 R1R2 R1R3 R2R3	crosshole crosshole crosshole crosshole	no no no no	2.4 2.4 2.4 2.4	3.5 3.5 3.5 3.5	2.5 2.5 2.5 2.5	83.6 75.4 75.4 75.4	62.1 58.2 58.2 58.2	sand & gravel	136 154 161 173	153 177 185 198	0.19 0.19 0.19 0.19	0.16 0.16 0.16 0.16	Barrow (1983); Bennett (1995); Bennett and Tinsley (1995)
Salinas River, north	SR1 R1R2 R1R3 R2R3	crosshole crosshole crosshole crosshole	no no no no	6.0 6.0 6.0 6.0	9.1 9.1 9.1 9.1	1.5 1.5 1.5 1.5	178.2 178.2 178.2 178.2	140.8 140.8 140.8 140.8	silty sand	177 195 200 199	162 179 184 183	0.15 0.15 0.15 0.15	0.11 0.11 0.11 0.11	
Salinas River, south	SR1 R1R2 R1R3 R2R3	crosshole crosshole crosshole crosshole	no no no no	6.0 6.0 6.0 6.0	6.5 6.5 6.5 6.5	4.5 4.5 4.5 4.5	142.2 142.2 142.2 142.2	123.5 123.5 123.5 123.5	sand & silty sand	131 149 158 168	124 141 150 159	0.15 0.15 0.15 0.15	0.11 0.11 0.11 0.11	

Table 1 (cont.) - Vs-based Liquefaction and Non-liquefaction Case Histories

(1)	(2)	(3)	(4)	(5)	(6)	(7)	(8)	(9)	(10)	(11)	(12)	(13)	(14)	(15)
Santa Cruz	SC02	SCPT	yes	0.6	1.3	2.6	48.1	28.7	sand to	116	160	0.42	0.44	Hryciw (1991)
	SC03	SCPT	yes	2.1	2.1	2.3	60.1	48.1	sandy silt	145	174	0.42	0.33	
	SC04	SCPT	no	1.8	1.8	2.2	51.0	41.0		126	158	0.42	0.33	
	SC05	SCPT	no	2.8	3.0	1.6	67.7	57.8		135	155	0.42	0.31	
	SC13	SCPT	no	1.8	2.0	4.0	69.2	49.8		158	188	0.42	0.36	
	SC14	SCPT	yes	1.2	1.4	1.6	41.0	30.5		126	170	0.42	0.37	
Moss Landing, State Beach	UC-15	SCPT	yes	1.8	1.8	2.8	63.6	46.9	Sand	116	140	0.25	0.21	Boulanger et al. (1995); Boulanger et al. (1997)
	UC-16	SCPT	yes	2.3	2.3	7.1	101.3	69.8		162	178	0.25	0.22	
Moss Landing, Sandholt Rd.	UC-4	SCPT	yes	1.8	2.1	1.5	54.2	42.4	Sand	130	161	0.25	0.20	
	UC-4	SCPT	no	1.8	5.9	4.1	148.5	87.7		209	216	0.25	0.26	
	UC-6	SCPT	marginal	1.7	3.0	4.3	85.6	59.5		171	196	0.25	0.22	
Moss Landing, Harbor Office	UC-12	SCPT	yes	1.9	3.0	1.6	74.8	53.1	Silty sand	150	175	0.25	0.22	
Moss Landing, Woodward Marine	UC-9	SCPT	yes	1.2	2.6	1.4	60.3	39.6	Sand	143	180	0.25	0.24	

(s) 1993 Hokkaido-nansei-oki, Japan Earthquake ($M_w = 8.3$)

Pension House	BH1	downhole	yes	1.0	1.0	2.5	45.5	33.4	sandy	79	105	0.19	0.16	Kokusho et al. (1995a, 1995b)
	BH2	downhole	marginal	0.7	3.7	4.8	122.9	70.0	gravel	144	159	0.19	0.21	

(t) 1995 Hyogo-ken Nanbu, Japan Earthquake ($M_w = 6.9$)

Port Island, instrumented array	1991	downhole	yes	2.4	2.4	12.6	160.8	98.8	sandy	197	202	0.50	0.43	Sato et al. (1996); Shibata et al. (1996); Sugito et al. (1996)
	1995	downhole	yes	2.4	2.4	12.6	185.9	110.9	gravel with silt	174	172	0.50	0.44	
SGK (TRC)		downhole	no	7.0	7.0	4.0	158.5	139.1	sand, silt	149	138	0.48	0.32	
TKS (TPS)		downhole	yes	2.5	2.5	4.6	73.8	57.9	gravel, sand, silt	135	157	0.20	0.15	
KNK (KPS)		downhole	no	2.0	3.8	13.2	193.6	111.0	sand, silt	179	184	0.12	0.10	

Test array refers to the two boreholes used for crosshole measurements, the borehole (or cone sounding) and source used for downhole measurements, or the line of receivers used for SASW measurements.

V_S is shear wave velocity and V_{S1} is shear wave velocity modified to an overburden pressure of 100 kPa using $V_{S1} = V_S (100 \text{ kPa} / \sigma'_v)^{0.25}$ (Robertson et al. 1992). Averages for the Treasure Island and Santa Cruz SCPT data are of the unfiltered data. One high velocity measurement is omitted from the average for Santa Cruz test array SC04. Refracted wave velocities measured at 5.5 m are omitted from the averages for Coyote Creek (test arrays R1R2, R1R3 and R2R3).

Average a_{max} is the average of two peak ground surface accelerations obtained from the x and y ground motion records that would have occurred at the site in the absence of liquefaction.

M_w is moment magnitude.

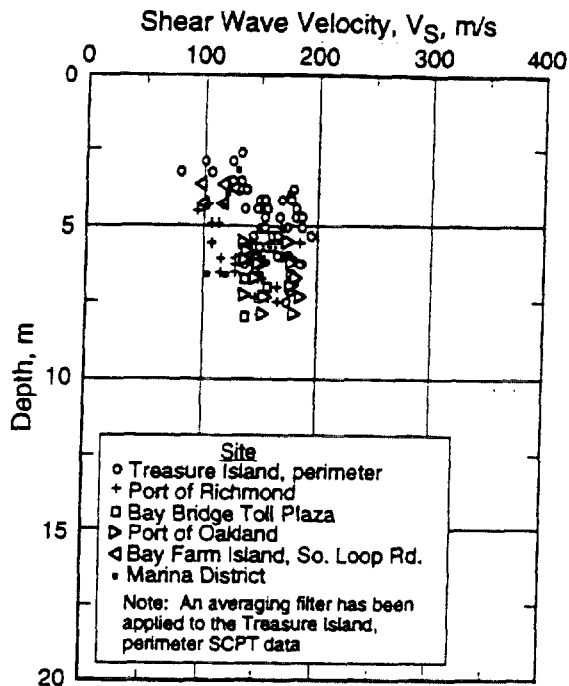
At Owi Island No. 1, Lotung LSST Facility, Sunamachi, Wildlife (1987 earthquakes), and Port Island sites the assessment of liquefaction or no liquefaction is supported by pore water pressure measurements.

At Larter Ranch and Whiskey Springs, soil may be weakly cemented by carbonate.

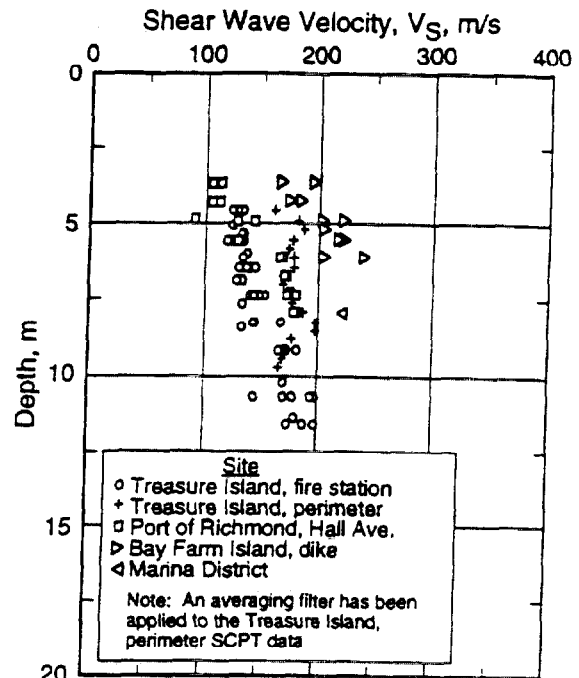
At Lotung LSST Facility, the artesian pressure is assumed to vary linearly from a pressure head of 8.1 m at a depth of 7 m to a pressure head of 1.9 m at a depth of 2 m.

At Treasure Island Fire Station, Moss Landing Sandholt Road UC-6, and Pension House BH2 no sand boils or damaged observed, although some liquefaction observed in adjacent areas. Thus, liquefaction behavior is listed as marginal for these sites.

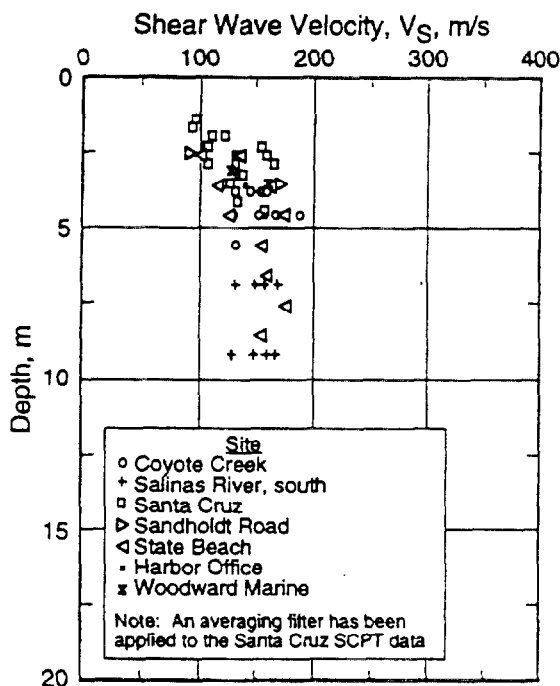
At Moss Landing Sandholt Road UC-4 no lateral displacement occurred below 5.9 m based on slope inclinometer data.



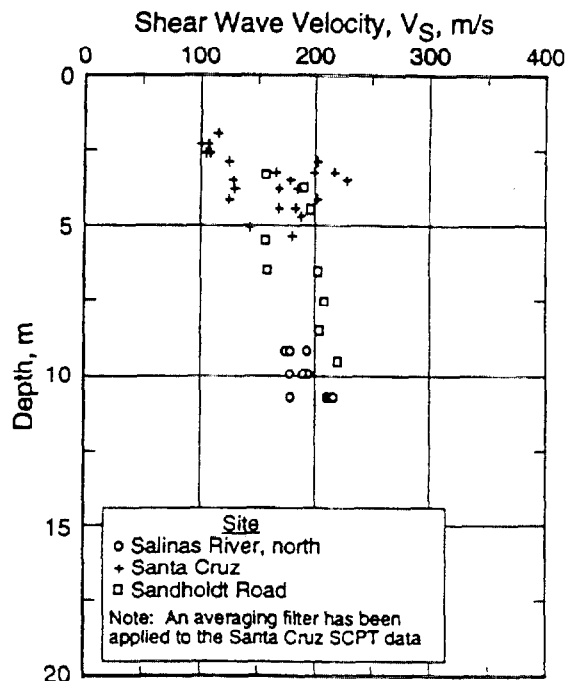
(a) Northern California Fill Sites Exhibiting Surface Manifestations of Liquefaction



(b) Northern California Fill Sites Not Exhibiting Surface Manifestations of Liquefaction

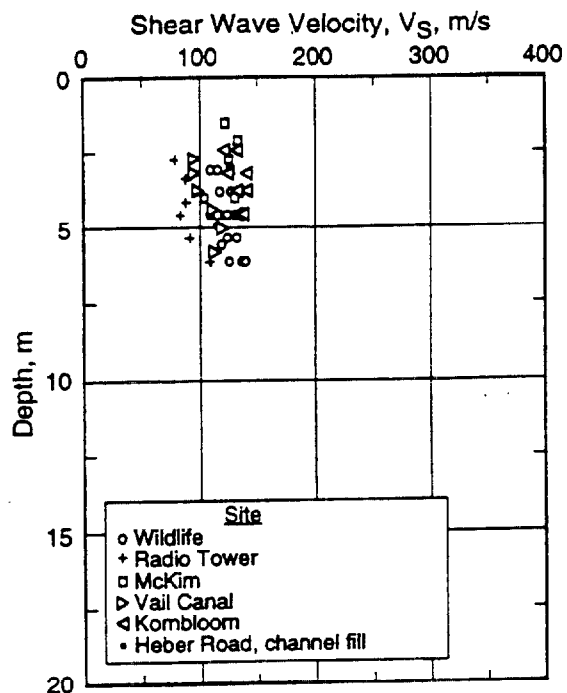


(c) Northern California Natural Soil Sites Exhibiting Surface Manifestations of Liquefaction

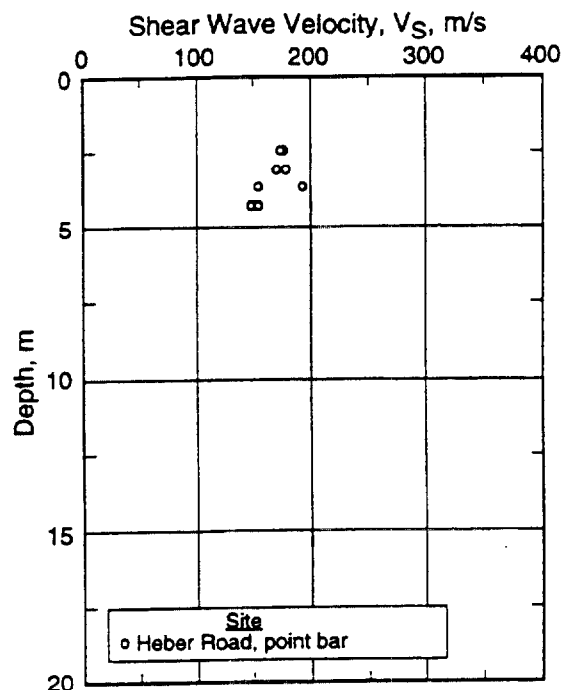


(d) Northern California Natural Soil Sites Not Exhibiting Surface Manifestations of Liquefaction

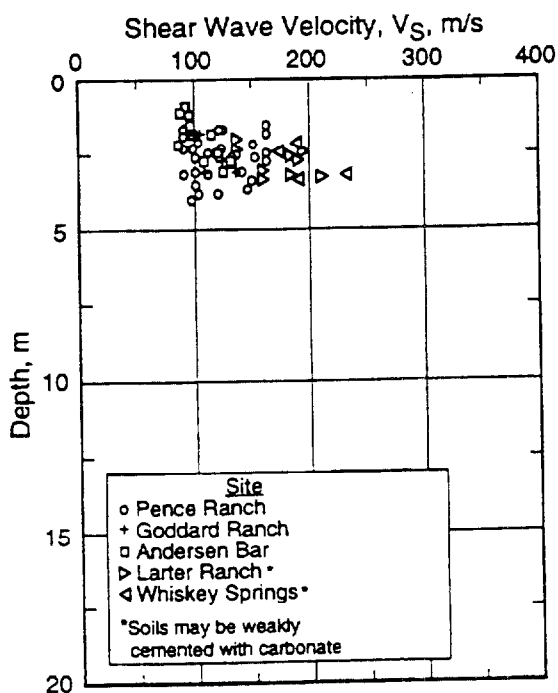
Fig. 1 - The Distribution of Shear Wave Velocity with Depth for the Most Vulnerable Layer at the Sites Listed in Table 1.



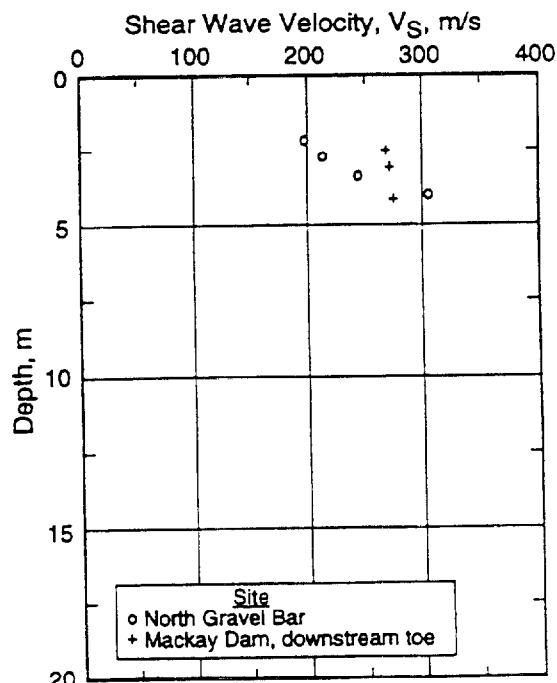
(e) Imperial Valley, California Sandy Soil Sites Exhibiting Surface Manifestations of Liquefaction



(f) Imperial Valley, California Sandy Sites Not Exhibiting Surface Manifestations of Liquefaction



(g) Idaho Gravelly Soil Sites Exhibiting Surface Manifestations of Liquefaction



(h) Idaho Gravelly Soil Sites Not Exhibiting Surface Manifestations of Liquefaction

Fig. 1 (cont.) - The Distribution of Shear Wave Velocity with Depth for the Most Vulnerable Layer at the Sites Listed in Table 1.

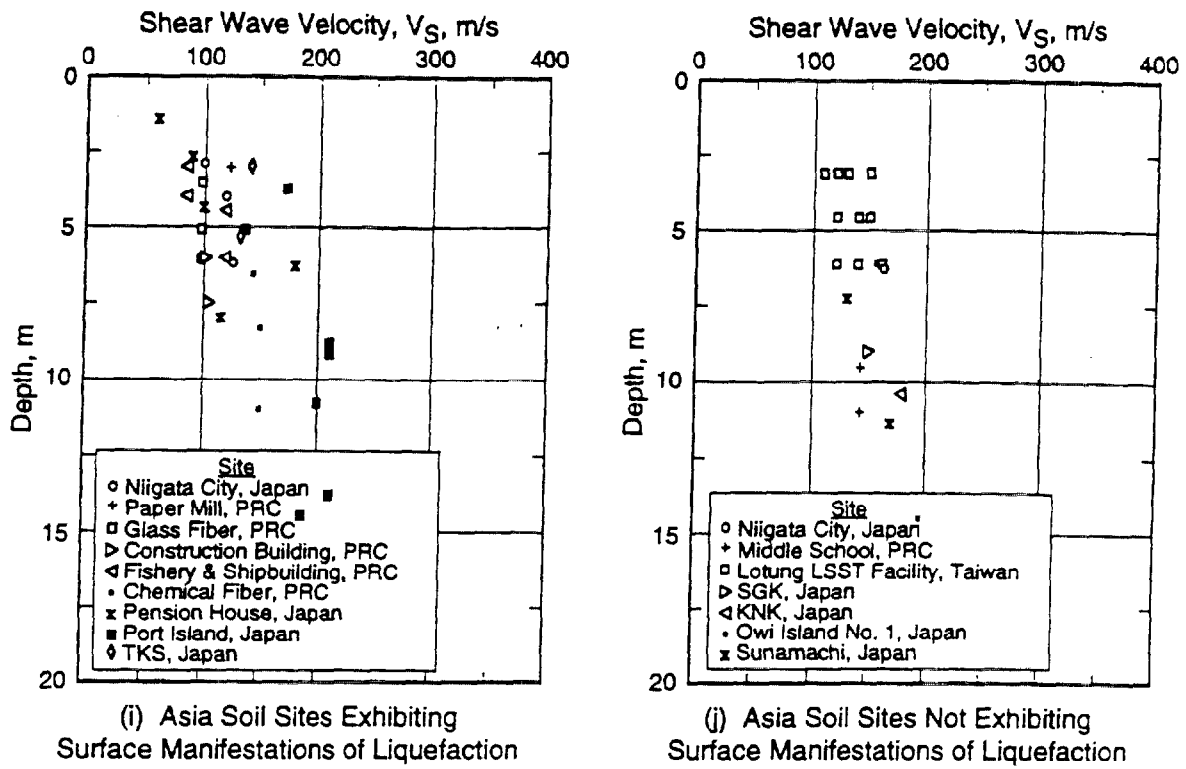


Fig. 1 (cont.) - The Distribution of Shear Wave Velocity with Depth for the Most Vulnerable Layer at the Sites Listed in Table 1.

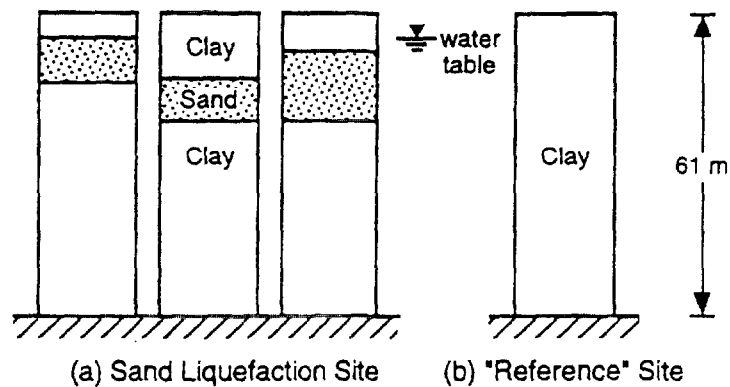


Fig. 2 - Soil Model Used in the Parametric Study by Stokoe et al (1988b).

were placed. The variations in shear modulus and material damping ratio with shearing strain assumed for the sand and clay layers were based on resonant column and cyclic triaxial tests on specimens from the Imperial Valley (Ladd 1982; Turner and Stokoe 1982).

Most of the analyses were performed (Bierschwale and Stokoe 1984; Aouad 1986) with the strong-motion acceleration time history which was recorded at the Salton Sea station during the 1981 Westmorland earthquake (moment magnitude, $M_w = 5.9$). This strong-motion record exhibited a peak horizontal ground surface acceleration, a_{max} , of 0.20 g and an equivalent number of cycles, N_c , of about 10. Records of larger magnitude were fabricated by simply multiplying the Salton Sea record by a pre-selected factor. Records with N_c of about 20 cycles and 30 cycles were generated by doubling and tripling the strong-motion portion of the Salton Sea record.

Stresses and strains within each soil profile were computed with program SHAKE (Schnabel et al. 1972), an equivalent linear analysis. These calculations were repeated with either a larger or smaller magnitude record until the estimated shearing strain within the liquefiable sand layer equaled the cyclic strain required for initial liquefaction. Initial liquefaction was assumed to occur at shearing strains of about 2%, 1% and 0.5% for 10 cycles, 20 cycles and 30 cycles of loading, respectively, based on undrained, strain-controlled cyclic triaxial tests on two Imperial Valley sands (Ladd 1982). The sand layer had been divided into 1.5-m thick sublayers, each having the same stiffness. The computed strain within the bottom sublayer was always greater than the computed strain in the other sublayers. Thus, criterion for initial liquefaction was first satisfied in the bottom sublayer. Next, the scaled record that generated initial liquefaction was applied at bedrock beneath the second profile, shown in Fig. 2b, to determine a_{max} at the ground surface of the non-liquefiable or "reference" soil site. These procedures were followed for each set of parameters characterizing the liquefiable sand layer (V_S , depth, and thickness). A total of 46 velocity profiles was considered.

Since it seemed more likely engineers would estimate a_{max} at the ground surface of non-liquefiable soil sites than at liquefiable sites, Stokoe et al. (1988b) correlated V_S of the liquefiable sand layer with a_{max} estimated for a "reference" soil site at the candidate-site location. The data from their parametric study are summarized in Figs. 3a, 3b and 3c for N_c of 10 cycles, 20 cycles and 30 cycles, respectively. As noted by Stokoe et al., the plotted data exhibit the following general trends: (1) the higher the V_S , the less likely the site is to liquefy for a given a_{max} ; (2) the greater the thickness of the liquefiable sand layer, the less likely the site is to liquefy for a given V_S ; and (3) the greater the depth to the bottom of the liquefiable sand layer, the slightly more likely the site is to liquefy at a given V_S . These findings suggest that liquefaction potential is dependent on layer thickness and depth, and indicate that a separating band (to allow for variations in thickness and depth) is more appropriate than a separating line to distinguish between liquefaction and non-liquefaction.

Stokoe et al. (1988b) created liquefaction assessment charts by dividing Figs. 3a, 3b and 3c each into three regions: the region left of the plotted data, the region of the plotted data, and the region right of the plotted data. Liquefaction is predicted to not occur left of the plotted data

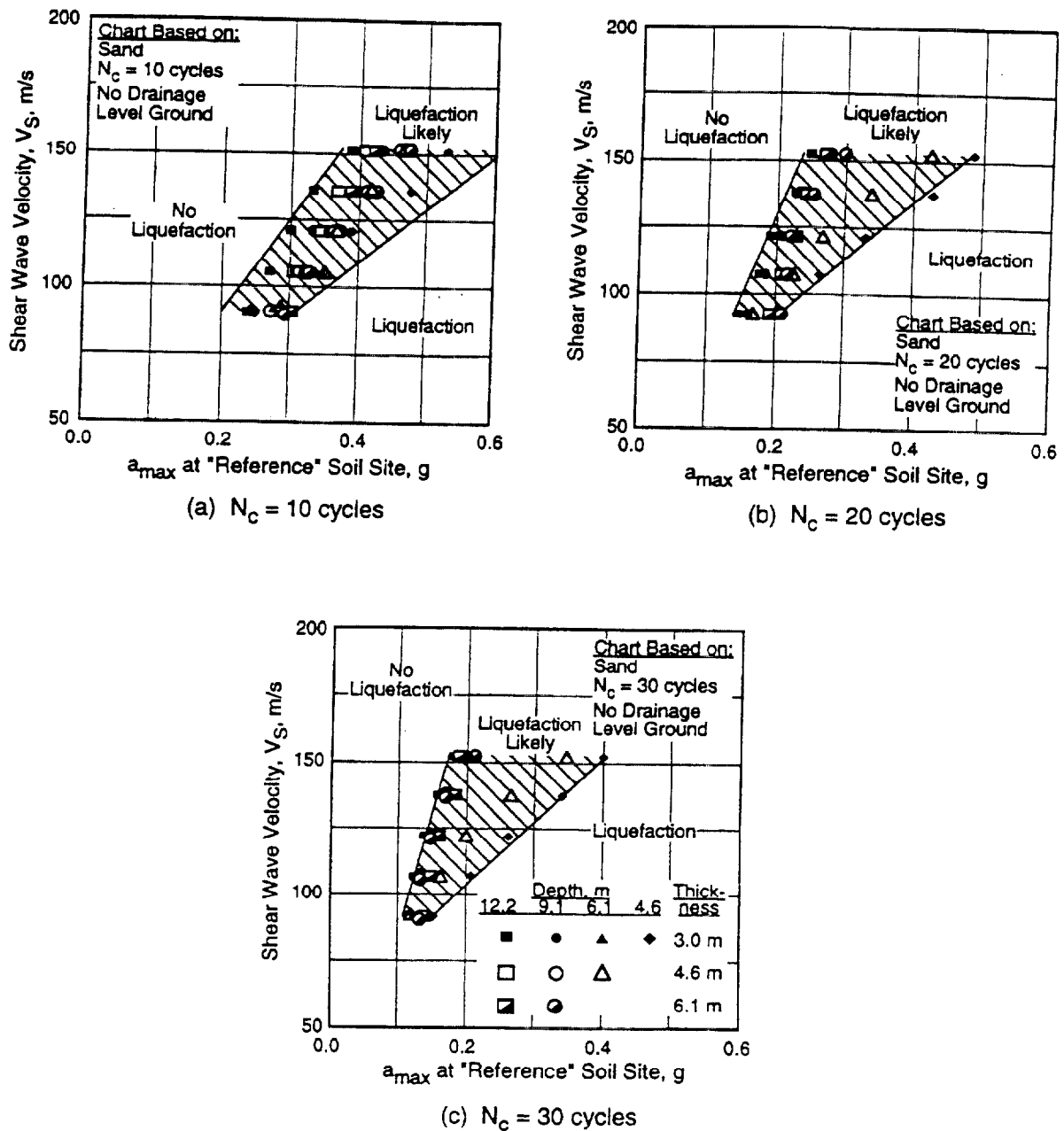


Fig. 3 - Comparison of Liquefaction Assessment Charts Proposed by Stokoe et al. (1988b) with Relationship Between V_S of Liquefiable Sand Layer and a_{max} for 10, 20 and 30 Cycles of Shaking as Determined Analytically by Bierschwale and Stokoe (1984) and Aouad (1986).

because the sand is too stiff to liquefy. Within the region of the plotted data, liquefaction would likely occur, but depends on layer thickness and depth. Right of the plotted data, liquefaction is predicted to occur.

To test the accuracy of these liquefaction assessment charts, field performance data for the magnitude 5.9 to 6.6 earthquakes listed in Table 1 are plotted on the chart for N_c of 10 cycles shown in Fig. 4a. The chart for N_c of 10 cycles is used since it was developed using a strong motion record from the magnitude 5.9 Westmorland earthquake. The field performance data for the magnitude 6.9 to 7.1 earthquakes are plotted on the chart for N_c of 15 cycles shown in Fig. 4b. For each case history, the shear wave velocity shown is the minimum measurement made within the most vulnerable layer. The value of a_{max} is for the larger of the x and y records of ground acceleration that would have occurred at the site in the absence of liquefaction. With several exceptions, the liquefaction (solid symbols) and non-liquefaction (open symbols) case histories are distinctly separated by the likely liquefaction region. Marginal liquefaction (half open symbols) is shown for the Chemical Fiber, Treasure Island Fire Station, and Sandholt Road UC-6 sites. Liquefaction behavior predicted by the procedure by Stokoe et al. (1988b) is nonconservative for lower levels of shaking ($a_{max} < 0.3$ g) and lower values of V_S ($V_S < 180$ m/s). A similar conclusion was reached by Arulanandan et al. (1986) based on the six sites shaken by the 1975 Haicheng earthquake listed in Table 1.

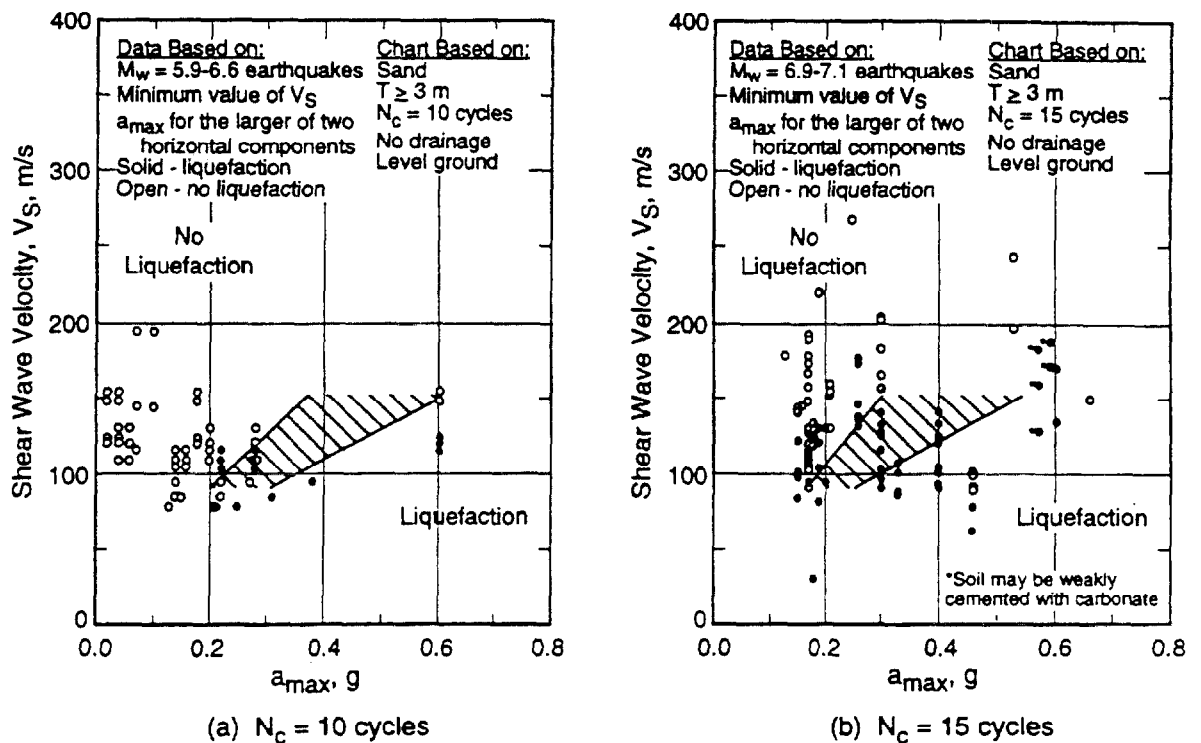


Fig. 4 - Comparison of Liquefaction Assessment Charts Proposed by Stokoe et al. (1988b) Based on V_S and a_{max} with Case Histories of Sites Shaken by Earthquakes with Magnitude of 5.9 to 7.1 (after Stokoe et al. 1988b; Andrus 1994).

While it has been suggested (Andrus 1994; after Robertson et al. 1992) that V_S be modified to a reference overburden stress, this modification alone does not improve the distribution of the performance data shown in Fig. 4. More work is needed to quantify the effects of layer thickness and depth.

Procedures Developed from Laboratory Studies

Tokimatsu et al. (1991a) proposed a procedure for evaluating liquefaction resistance using the stress approach developed by Seed and his colleagues (1971, 1983, and 1985) and results from laboratory cyclic triaxial tests on reconstituted sand specimens. In the stress approach, cyclic loading is represented by the ratio of cyclic shear stress to initial vertical effective stress acting on a horizontal plane, called cyclic stress ratio. The cyclic stress ratio, CSR, at a particular depth in a level soil deposit can be expressed as (Seed and Idriss 1971):

$$CSR = \tau_{av}/\sigma'_v = 0.65 (a_{max}/g) (\sigma_v/\sigma'_v) r_d \quad (1)$$

where τ_{av} is average cyclic shear stress generated by the earthquake, σ'_v is initial effective vertical (overburden) stress, σ_v is total overburden stress, g is acceleration of gravity, and r_d is a shear stress reduction factor with a value less than 1.

Resistance to liquefaction in a soil deposit is represented by a cyclic stress ratio or cyclic resistance ratio, CRR. Tokimatsu et al. (1991a) defined the cyclic resistance ratio for cyclic triaxial tests, CRR_{tx} , as the ratio of cyclic deviator stress to initial effective confining stress, $\sigma_d/2\sigma'_o$, at the time the double-amplitude axial strain, DA, reaches 5%. Their correlations between CRR_{tx} at different number of cycles and stress corrected shear wave velocity, V_{S1} , are shown in Fig. 5. They used the assumption that V_S is a function of the cube root of the mean normal effective stress, σ'_m , and corrected V_S by:

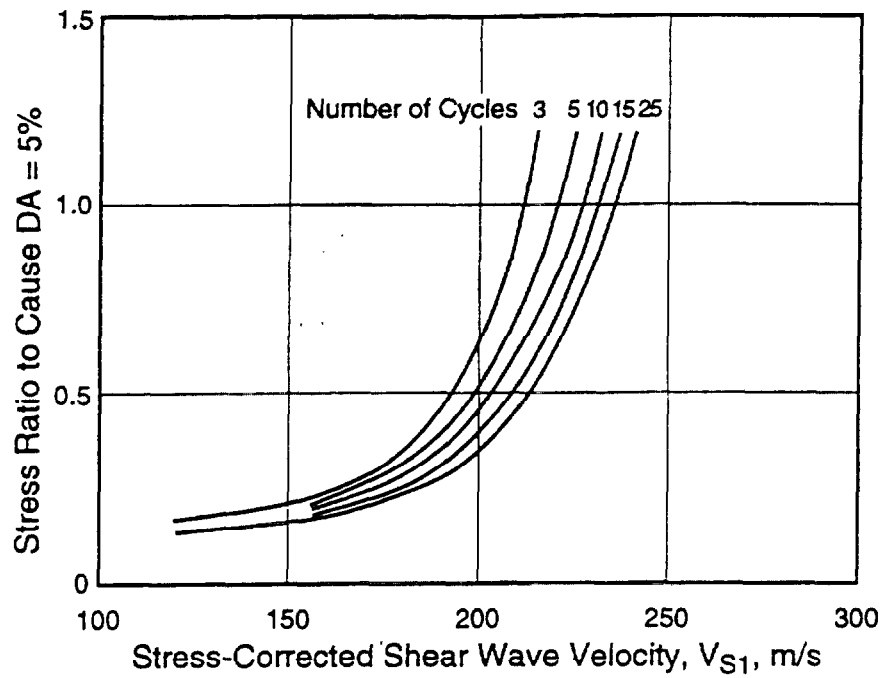
$$V_{S1} = V_S (1/\sigma'_m)^{0.33} \quad (2)$$

where σ'_m is in kgf/cm^2 ($1 \text{ kgf/cm}^2 = 98.07 \text{ kPa}$). Tokimatsu et al. selected an exponent of 0.33 rather than 0.25, as determined by Hardin and Drnevich (1972), because it seemed that a slightly better correlation could be obtained.

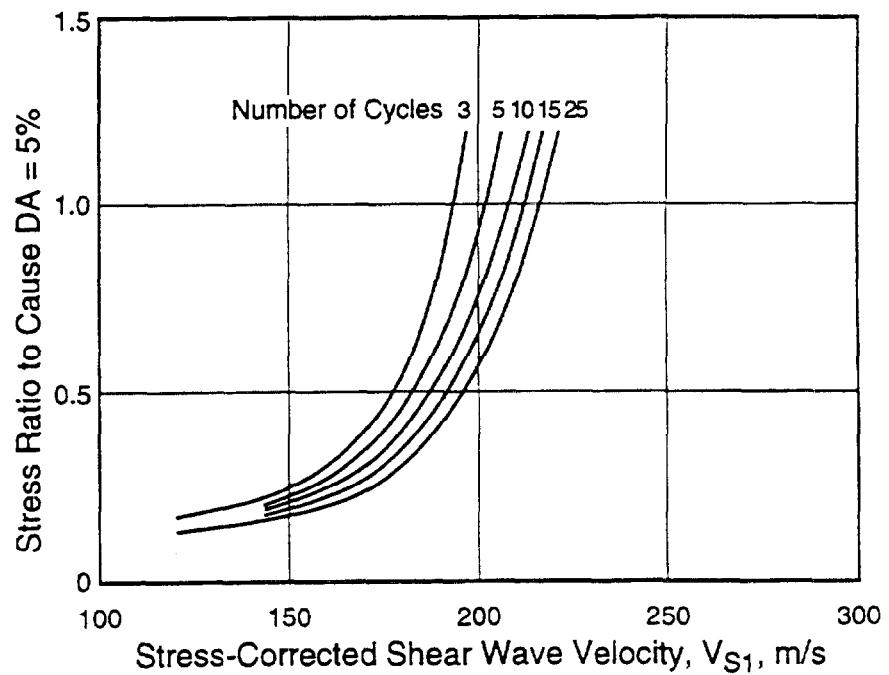
For converting CRR_{tx} to an equivalent field cyclic resistance ratio, Tokimatsu et al. (1991a) suggested the following expression (after Seed 1979):

$$CRR = \tau_l/\sigma'_v = 1/3 (1+2K_o) r_c (CRR_{tx}) \quad (3)$$

where τ_l is average cyclic shear stress resisting liquefaction, K_o is the coefficient of earth pressure at rest, and r_c is a constant to account for the effects of multidirectional shaking with a value between 0.9 and 1.0. As noted by Tokimatsu et al., any value of K_o between 0.5 and 1 can be assumed for all practical purposes since the effects involved in Eqs. 2 and 3 almost cancel each other out.



(a) Clean Sand



(b) Silty Sand

Fig. 5 - Liquefaction Assessment Charts Based on V_{S1} Proposed by Tokimatsu et al. (1991a).

The field performance data for 20 earthquakes are plotted in Fig. 6. The plotted data are based on the procedure of Tokimatsu et al. (1991a) outlined above using minimum values of V_{S1} from the most vulnerable layer and estimates of a_{max} for the larger of the x and y records of ground acceleration that would have occurred at the site in the absence of liquefaction. Included in Fig. 6 are the liquefaction potential boundaries by Tokimatsu et al. The boundaries are constructed from the relationships shown in Fig. 5 using Eq. 3 and assuming K_o of 0.6 and r_c of 0.95. Liquefaction behavior predicted by these boundaries is nonconservative for N_c greater than about 10 cycles and V_{S1} greater than about 150 m/s (see Figs. 6c and 6d).

Procedures Developed from Field Performance Studies

Robertson et al. (1992) proposed another stress-based liquefaction assessment procedure using field performance data from primarily the Imperial Valley, California sites. They corrected V_S by:

$$V_{S1} = V_S (P_a / \sigma'_v)^{0.25} \quad (4)$$

where P_a is a reference stress, 100 kPa or approximately atmospheric pressure, and σ'_v is in kPa. Robertson et al. chose to correct V_S in terms of σ'_v to follow the traditional procedures for correcting standard and cone penetration resistances. It is implied by Eq. 4 that K_o equals 1, since V_S is a function of mean effective stress (Hardin and Drnevich 1972). Their liquefaction potential boundary for earthquakes with magnitude of 7.5 is shown in Fig. 7a.

Two subsequent liquefaction potential boundaries proposed by Kayen et al. (1992) and Lodge (1994) for earthquakes with magnitude of about 7 are shown in Fig. 7b. These later curves are based on field performance data from primarily the 1989 Loma Prieta, California earthquake. Kayen et al. used field performance data from the Port of Richmond, Bay Bridge Toll Plaza, Port of Oakland, and Bay Farm Island sites. They assumed average values of V_{S1} and a_{max} for the larger component of acceleration time histories recorded at neighboring seismograph stations.

Lodge (1994) considered the same sites that Kayen et al. (1992) evaluated as well as several additional sites that had been shaken by the Loma Prieta earthquake. The boundary by Lodge was developed as follows. First, cyclic stress ratios for the entire soil profile at each site were calculated using Eq. 1 and a_{max} for the larger component of acceleration time histories recorded at neighboring seismograph stations. Second, soil layers with a high and a low liquefaction potential were identified with the simplified procedure of Seed et al. (1985) and SPT blow counts. Soil layers where the modified blow count fell within 3 blows per 0.3 m of the SPT-based liquefaction potential boundary of Seed et al. were eliminated due to uncertainties in the correlation. Third, shear wave velocity measured by the SCPT and crosshole methods were normalized using Eq. 4. Fourth, on a "meter by meter" basis values of V_{S1} and cyclic stress ratio were plotted for both layer types, those which were predicted liquefiable and those which were predicted non-liquefiable. Finally, a curve was drawn to include all data for liquefiable layers.

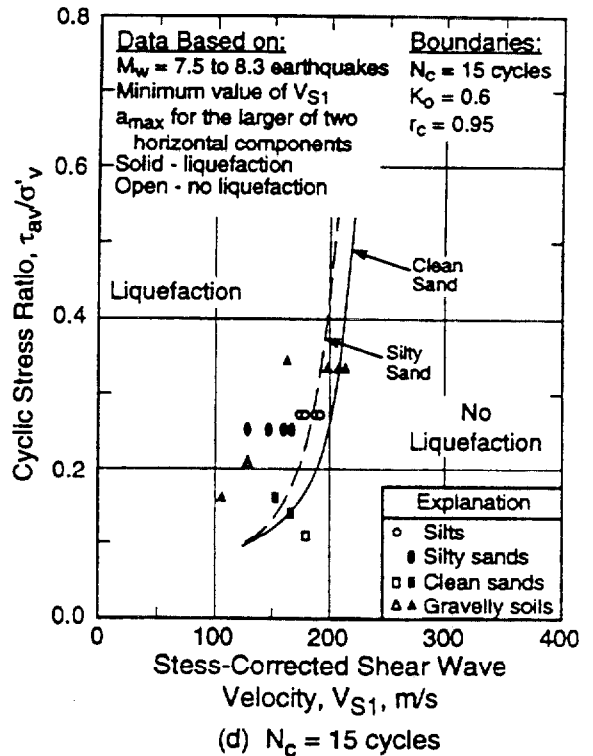
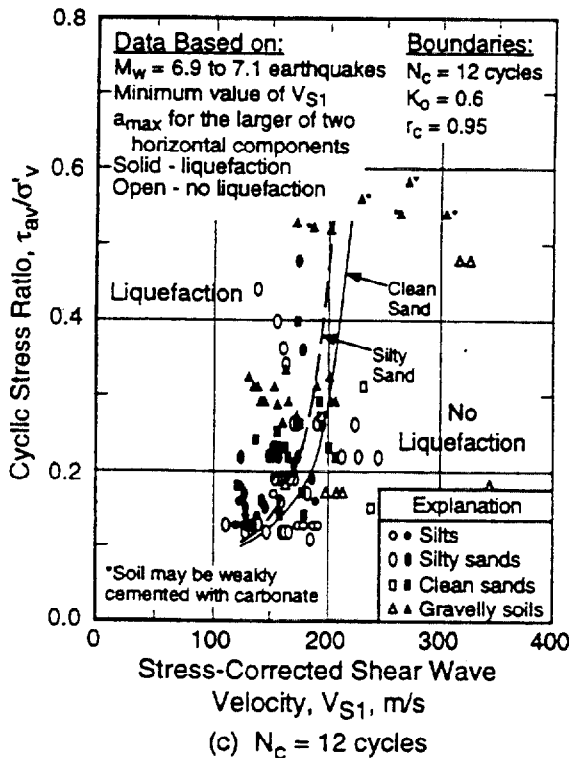
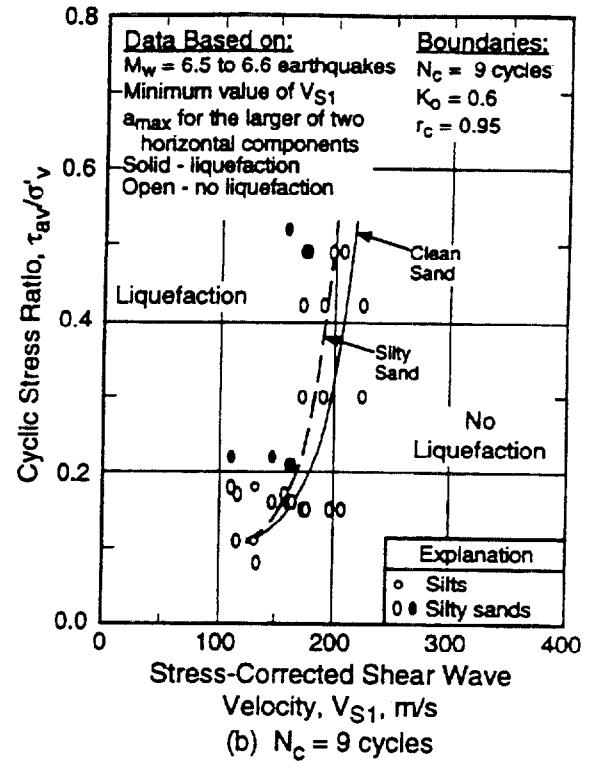
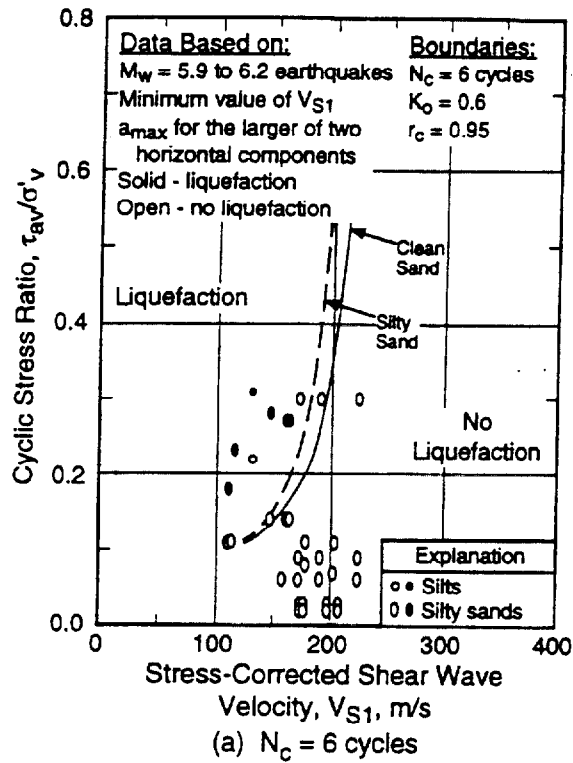


Fig. 6 - Comparison of Liquefaction Assessment Charts Based on V_{S1} and CSR Proposed by Tokimatsu et al. (1991a) with Case Histories from 20 Earthquake

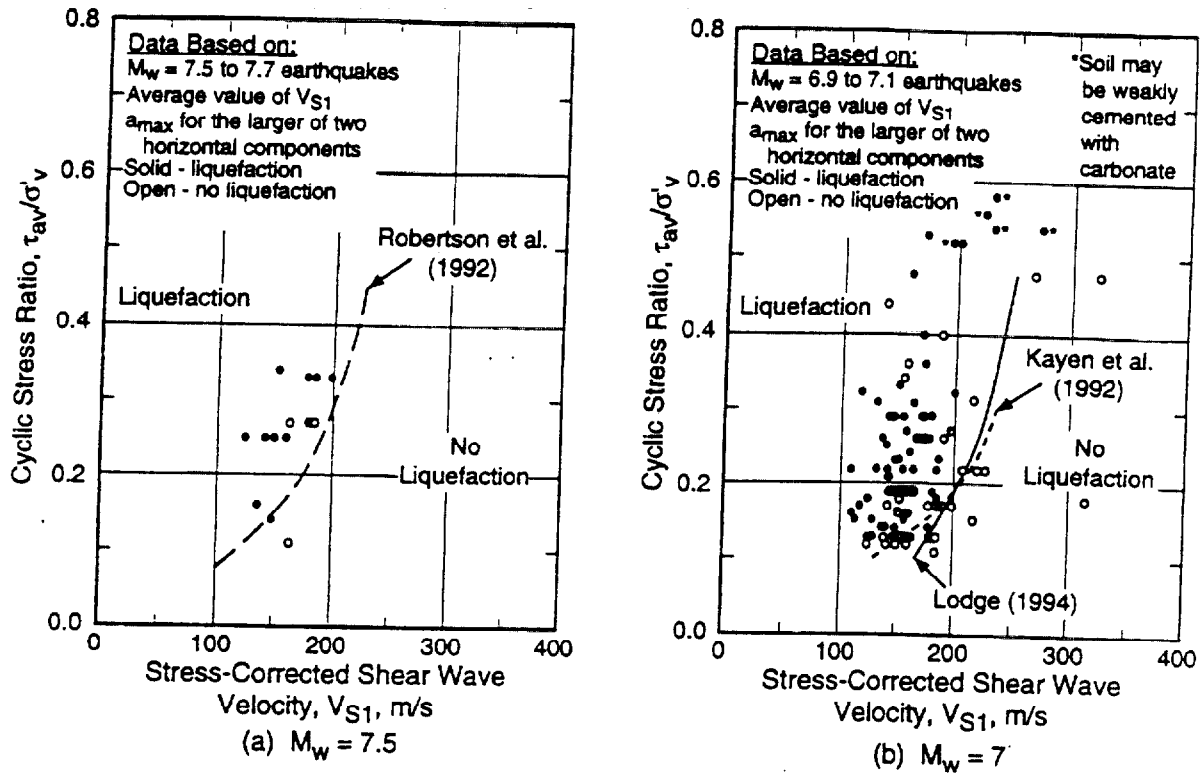


Fig. 7 - Comparison of Liquefaction Assessment Charts Based on V_{S1} and CSR Proposed by (a) Robertson et al. (1992) and (b) Kayen et al. (1992) and Lodge (1994) with Case Histories from Earthquakes with Magnitude of 6.9 to 7.7.

Field performance data from earthquakes with magnitude of 6.9 to 7.7 are also plotted in Fig. 7. The plotted data are based on average values of V_{S1} from the most vulnerable layer at the investigated sites. The cyclic stress ratios are calculated using estimates of a_{max} for the larger of two horizontal components of ground acceleration that would have occurred at the site in the absence of liquefaction. With a few exceptions, the liquefaction case histories are bounded by the relationships by Kayen et al. (1992) and Lodge (1994). The relationship by Robertson et al. (1992) is the least conservative of the three relationships.

Recommended Liquefaction Potential Boundaries Based on V_{S1} and CRR

After reviewing the proposed procedures outlined above, this workshop agreed that a careful review of the case histories should be conducted. It was suggested that the recommended V_{S1} -based procedure follow the general format of the CPT- and SPT-based procedures.

The compiled case histories for magnitude 5.9 to 7.7 earthquakes are shown in Figs. 8, 9 and 10. The plotted data have been separated into three categories: (1) sands and gravels with average fines (particles smaller than 75 μm) content less than or equal to 5%, Fig. 8; (2) sands and gravels with average fines content of 6% to 34%, Fig. 9; and (3) sands and silts with average fines content greater than or equal to 35%, Fig. 10. Where possible, the fines content is noted next to the data point corresponding to soils with over 5% fines. The data for the Larter Ranch and Whiskey Springs sites are not shown, since the soils at these two sites may be weakly cemented with carbonate. Following the recommendation of this workshop, the plotted data are based on representative values of V_{S1} and a_{max} for the average of peak values for the x and y ground acceleration time histories that would have occurred at the site in the absence of liquefaction. Values of V_{S1} are calculated using Eq. 4. Values of r_d are estimated using the relationship by Seed and Idriss (1971).

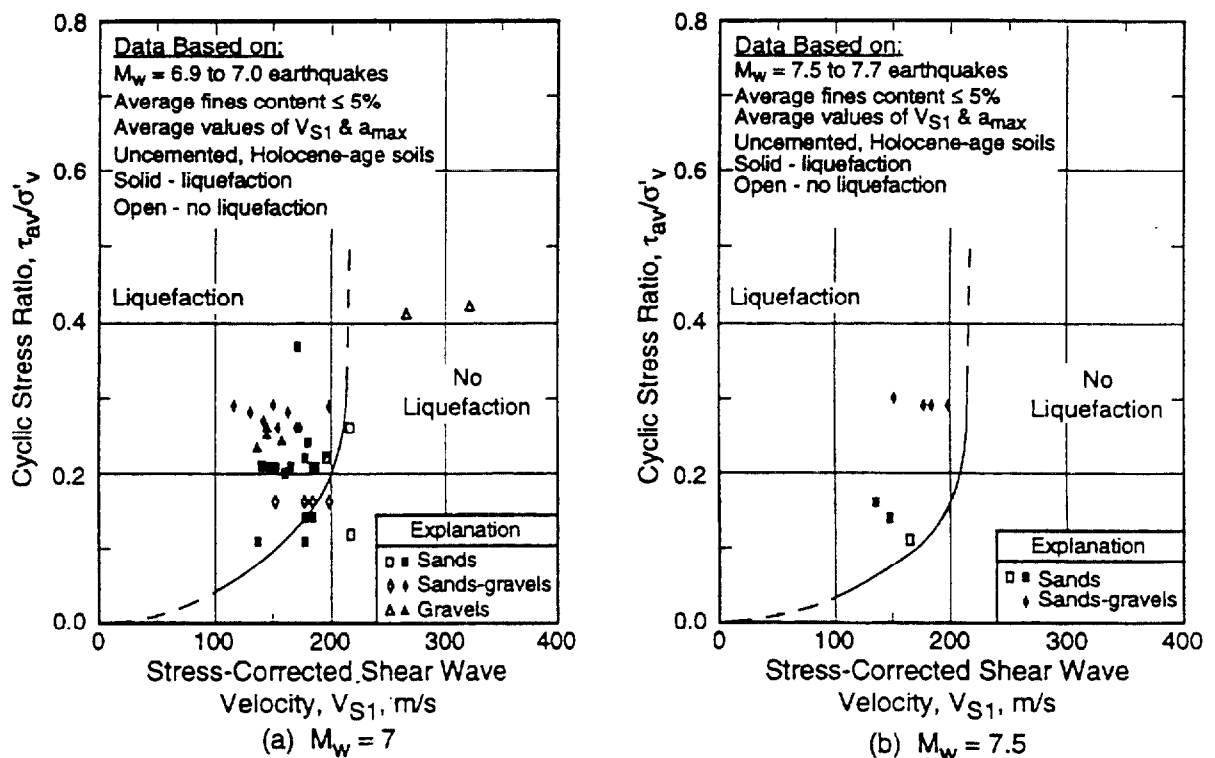


Fig. 8 - Comparison of Liquefaction Assessment Charts Based on V_{S1} and CSR from Analysis for this Report with Case Histories of Uncemented Soils with Fines Content Less than or Equal to 5%.

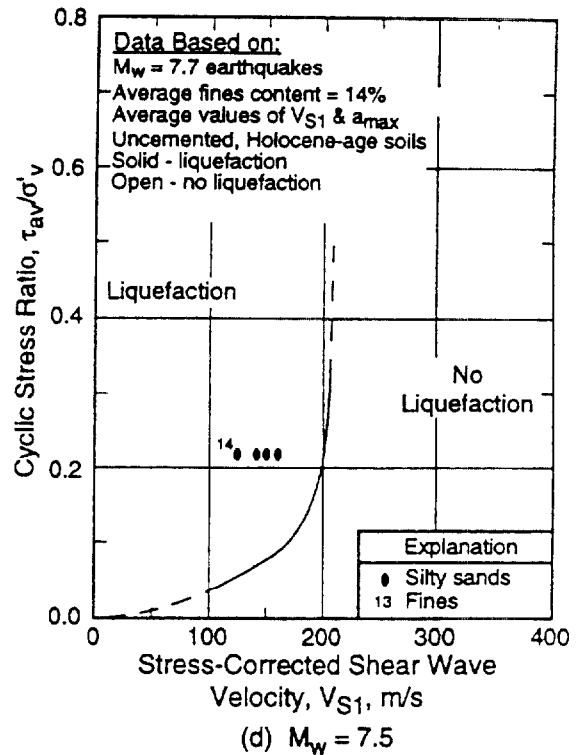
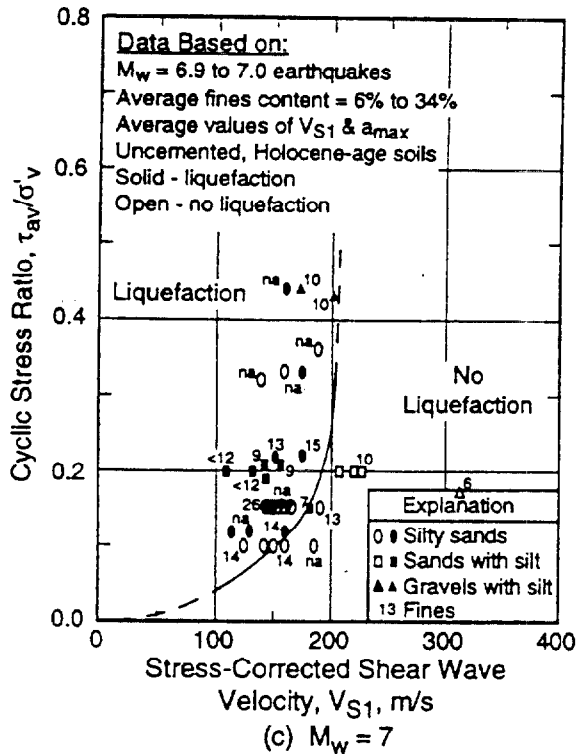
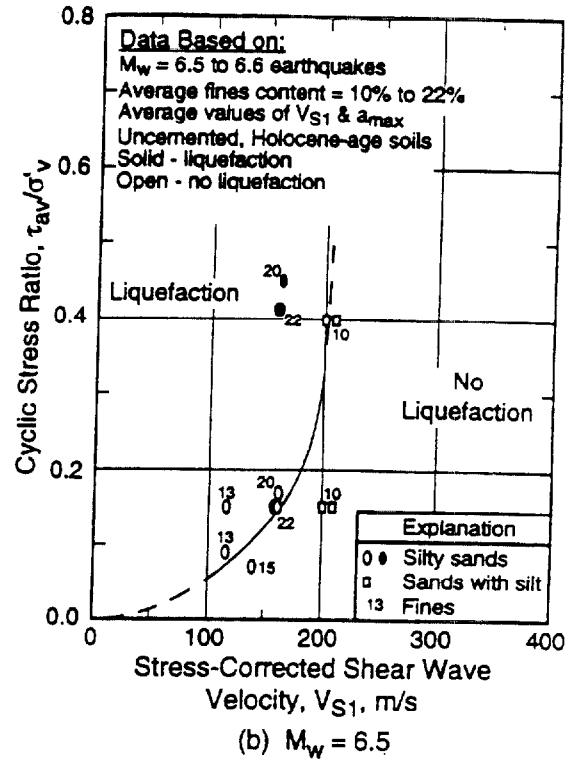
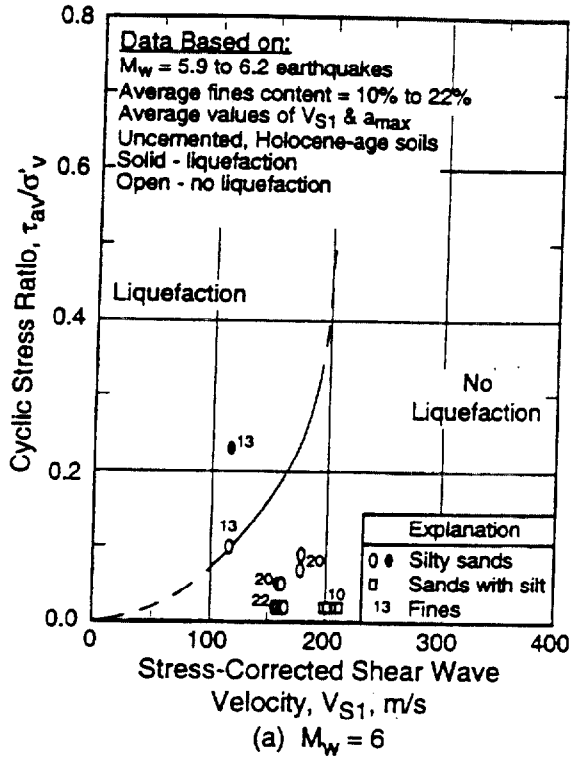


Fig. 9 - Comparison of Liquefaction Assessment Charts Based on V_{S1} and CSR from Analysis for this Report with Case Histories of Uncemented Soils with Fines Content of 6% to 34%.

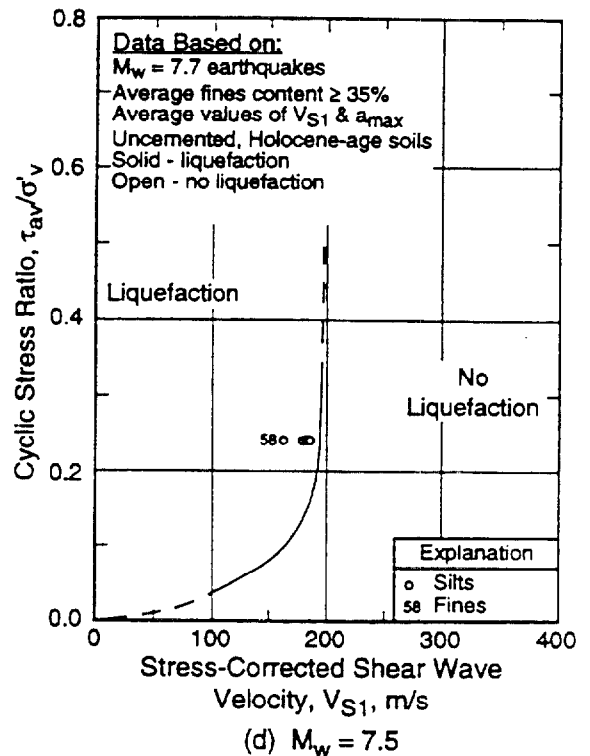
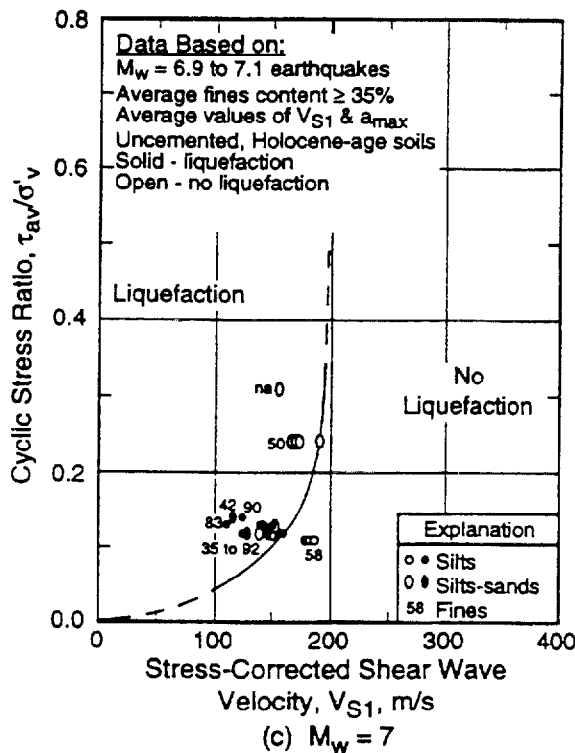
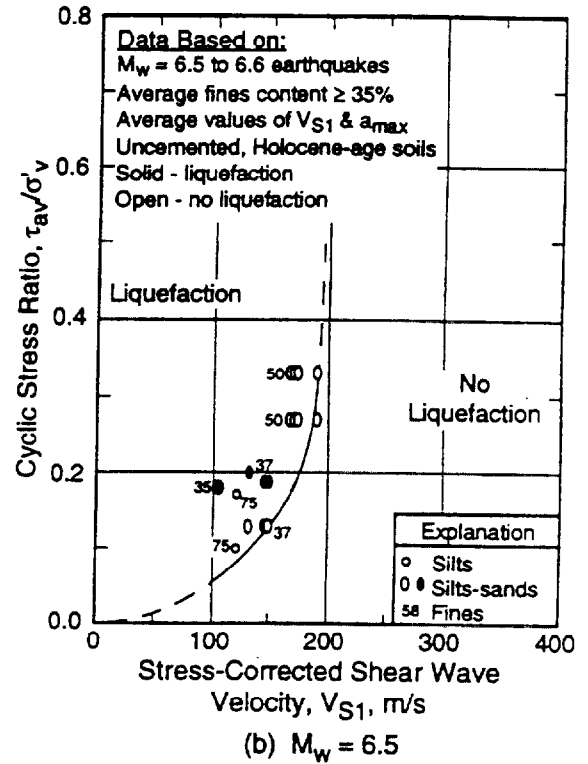
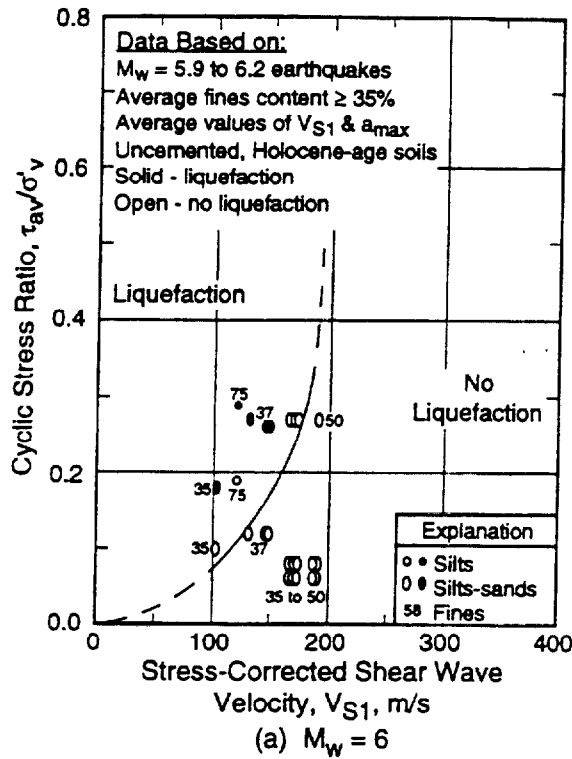


Fig. 10 - Comparison of Liquefaction Assessment Charts Based on V_{S1} and CSR from Analysis for this Report with Case Histories of Uncemented Soils with Fines Content Greater than or Equal to 35%.

Dobry (1996) derived a relationship between cyclic stress ratio and V_{S1} for constant average cyclic strain, γ_{av} , using the equations:

$$\gamma_{av} = \tau_{av}/(G)_{\gamma_{av}} \quad (5)$$

and

$$G_{max} = \rho V_S^2 \quad (6)$$

where $(G)_{\gamma_{av}}$ is shear modulus at γ_{av} , G_{max} is small-strain shear modulus, and ρ is mass density. Combining Eqs. 5 and 6, and dividing both sides by σ'_v leads to:

$$\tau_{av}/\sigma'_v = (\rho/\sigma'_v) \gamma_{av} (G/G_{max})_{\gamma_{av}} V_S^2 \quad (7)$$

If everything is done at a reference stress, P_a , then $V_S = V_{S1}$ and a line of constant average cyclic strain is of the form:

$$\tau_{av}/\sigma'_v = f(\gamma_{av}) V_{S1}^2 \quad (8)$$

where $f(\gamma_{av}) = (\rho/P_a) \gamma_{av} (G/G_{max})_{\gamma_{av}}$. This formulation assumes the modulus reduction factor, $(G/G_{max})_{\gamma_{av}}$, is independent of confining pressure and pore water pressure buildup. Equation 8 is strong evidence for extending the liquefaction potential boundaries to the origin, and provides a rational approach for establishing the boundaries at low values of V_{S1} (say $V_{S1} \leq 125$ m/s).

For higher values of V_{S1} , it seems reasonable that the boundary separating liquefiable and non-liquefiable soils would become asymptotic to some limiting value of V_{S1} . This limit is caused by the tendency of dense granular soils to exhibit dilative behavior at large strains. Thus, Eq. 8 is modified to:

$$CRR = \tau_i/\sigma'_v = a (V_{S1}/100)^2 + b [1/(V_{S1c} - V_{S1}) - 1/V_{S1c}] \quad (9)$$

where V_{S1c} is the critical value of V_{S1} that separates contractive and dilative behavior, and "a" and "b" are curve fitting parameters.

Using the relationship between CRR and V_{S1} expressed by Eq. 9, curves have been drawn to separate the liquefaction and non-liquefaction case histories plotted in Figs. 8, 9 and 10. The curves are drawn assuming $a = 0.03$ and $b = 0.9$ for earthquakes with magnitude of 7.5. Depending on fines content (FC), the following values of V_{S1c} are also assumed:

$$V_{S1c} = 220 \text{ m/s for sands and gravels with FC} \leq 5\% \quad (10a)$$

$$V_{S1c} = 210 \text{ m/s for sands and gravels with FC} \approx 20\% \quad (10b)$$

$$V_{S1c} = 200 \text{ m/s for sands and silts with FC} \geq 35\% \quad (10c)$$

For earthquakes with magnitude of 6, 6.5 and 7, scaling factors of 2.1, 1.6 and 1.25, respectively, are applied to the curves for magnitude 7.5 earthquakes. The curves shown in Figs. 8, 9 and 10 correctly predict more than 95% of the occurrences of liquefaction.

The three liquefaction case histories that lie slightly below the boundary curves shown in Figs. 8a and 9c are for the Treasure Island UM06 and UM11, and Marina District School sites. The data point for Treasure Island UM11 (see Fig. 9c) would lie on the boundary for 7% fines content, the average fines content of the most vulnerable layer for this site. In addition, the Treasure Island sites are located along the perimeter of the island where liquefaction was moderate during the 1989 Loma Prieta earthquake and where sloping ground may have been a factor. The Marina District School site is located on the margin of mapped artificial fill and liquefaction damage caused by the Loma Prieta earthquake. Hence, there are only two cases of liquefaction that incorrectly lie outside the region of predicted liquefaction as defined by these procedures, and they are cases of marginal to moderate liquefaction.

Figure 11 presents the recommended liquefaction potential boundaries for magnitude 7.5 earthquakes and uncemented Holocene-age soils with various fines content. Although these boundaries pass through the origin, natural alluvial sandy soils with shallow water tables rarely have stress corrected shear wave velocities less than 100 m/s, as shown by the in situ measurements presented in Figs. 8, 9 and 10. For a V_{S1} -value of 100 m/s and a magnitude 7.5 earthquake, the calculated CRR is 0.03. This minimal CRR value is consistent with intercept CRR values of 0.03 to 0.05 suggested by the CPT and SPT procedures. The recommended boundary for uncemented soils with fines content $\leq 5\%$ and earthquakes with magnitude of 7, shown in Fig. 8a, is similar to the boundaries of Kayen et al. (1992) and Lodge (1994), shown in Fig. 7b, at lower values of V_{S1} ($V_{S1} < 200$ m/s).

Values of V_{S1c} between 200 m/s and 220 m/s are consistent with values determined using the relationship between SPT blow count and shear wave velocity by Ohta and Goto (1976) modified to blow count with theoretical free-fall energy of 60% (Seed et al. 1985). Assuming a corrected blow count of 30 and a depth of 10 m, approximate values of V_{S1} range from 190 m/s for clays to 220 m/s for sandy gravels of Holocene-age. More work is needed to further validate and refine the values of V_{S1c} .

The magnitudes scaling factors of 2.1, 1.6 and 1.25 for earthquakes with magnitude of 6, 6.5 and 7, respectively, compare well with SPT-based factors developed in recent years by several investigators (Youd and Noble in press), as noted in Columns 3 through 7 of Table 2. They form the upper bound of scaling factors recommended by this workshop (Section 1, workshop report) for earthquakes with magnitude less than 7.5. The lower bound of the range of recommended scaling factors is defined by the scaling factors developed by Idriss (1996), as listed in Column 3 of Table 2.

The relationship between earthquake magnitude and magnitude scaling factor, MSF, can be expressed by (modified from Idriss 1996):

$$MSF = (M_w/7.5)^n \quad (11)$$

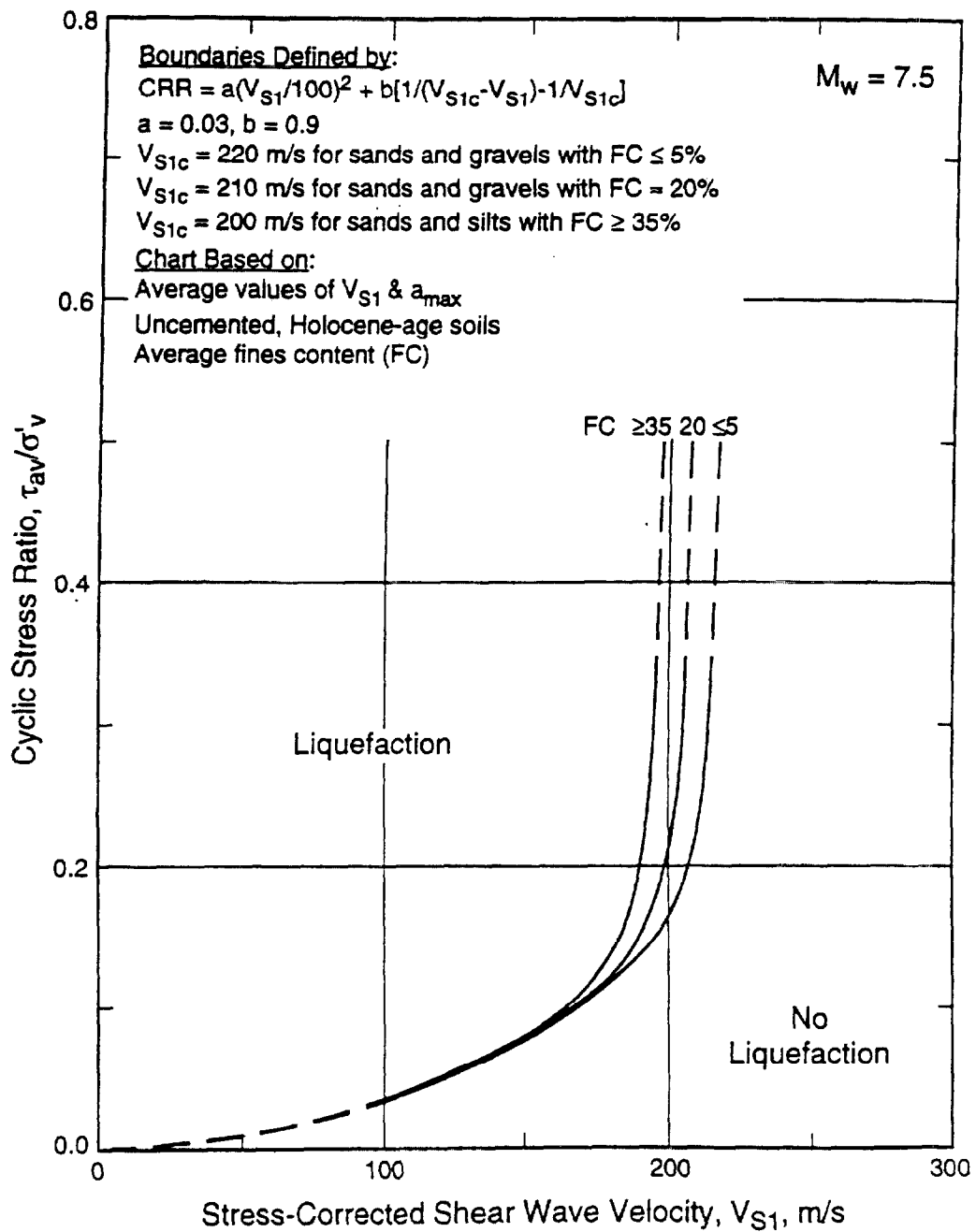


Fig. 11 - Recommended Liquefaction Assessment Chart Based on V_{S1} and CSR for Magnitude 7.5 Earthquakes and Uncemented Soils of Holocene Age.

where "n" is a curve fitting parameter. The scaling factors developed by Prof. Idriss as listed in Column 3 of Table 2 are defined by Eq. 11 with $n = -2.56$. For the scaling factors used to construct the V_S -based liquefaction potential boundaries shown in Figs. 8, 9 and 10 ($MSF = 2.1, 1.6, 1.25,$ and 1.0 for $M_w = 6, 6.5, 7$ and $7.5,$ respectively), the value of "n" is -3.3 .

While only the scaling factors determined by Idriss (1996) for earthquakes with magnitude greater than 7.5 have been recommended by this workshop, the scaling factors determined using $n = -3.3$ are slightly more conservative. For example, Eq. 11 with $n = -3.3$ provides scaling factors of 0.81 and 0.66 for earthquakes with magnitude of 8 and 8.5, respectively. These scaling factors are slightly less than the scaling factors of 0.84 and 0.72 for earthquakes with magnitude of 8 and 8.5, respectively, determined by Prof. Idriss.

Using Eq. 11 with $n = -3.3$ and the boundary for uncemented clean sands and gravels shown in Fig. 11, leads to the family of curves shown in Fig. 12. The curves shown in Fig. 12 imply that liquefaction will never occur in any earthquake if V_{S1} exceeds 220 m/s and the soils are uncemented and of Holocene age.

In areas with cemented soils, local correlations between shear wave velocity and penetration resistance should be developed to determine the effects of cementation. The boundaries shown in Fig. 11 could then be modified by increasing the abscissas by some factor. For example, measurements from the Larter Ranch and Whiskey Springs sites which liquefied during the 1983 Borah Peak, Idaho earthquake suggest a correction factor of about 1.3 to 1.4 (Andrus 1994) for those distal alluvial fan sediments.

Table 2. Magnitude Scaling Factors Obtained by Various Investigators (modified from Youd and Noble in press).

Moment Magnitude, M_w	Magnitude Scaling Factor (MSF)						This Report
	Seed and Idriss (1982)	Idriss (1996)	Ambraseys (1988)	Youd and Noble, $p < 32\%$ (in press)	Arango (1996)		
(1)	(2)	(3)	(4)	(5)	(6)	(7)	(8)
5.5	1.43	2.20	2.86	3.42	3.00	2.20	2.8*
6.0	1.32	1.76	2.20	2.35	2.00	1.65	2.1
6.5	1.19	1.44	1.69	1.66	1.60	1.40	1.6
7.0	1.08	1.19	1.30	1.20	1.25	1.10	1.25
7.5	1.00	1.00	1.00		1.00	1.00	1.0
8.0	0.94	0.84	0.67		0.75	0.85	0.8*
8.5	0.89	0.72	0.44				0.65*

*Extrapolated from scaling factors for $M_w = 6, 6.5, 7$ and 7.5 using $MSF = (M_w/7.5)^{-3.3}$.

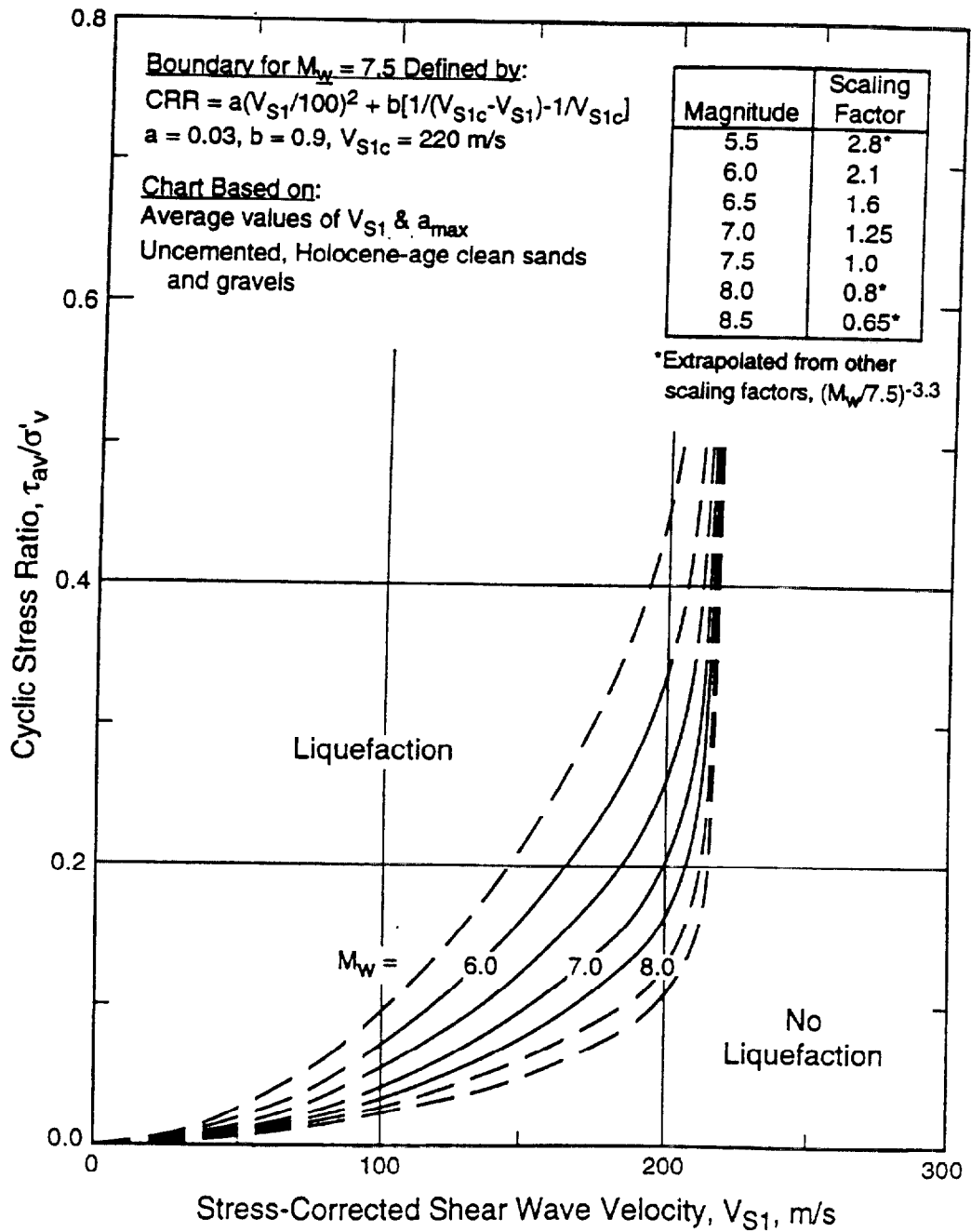


Fig. 12 - Recommended Chart Based on V_{S1} and CSR for Evaluation of Liquefaction Potential of Uncemented Clean Sands and Gravels of Holocene Age.

Recommended Liquefaction Potential Boundaries Based on V_S and a_{max}

By combining Eqs. 1, 4 and 9, a relationship based on V_S and a_{max} is obtained in the form of:

$$a_{max}/g = f_1 \{a (f_2 V_S/100)^2 + b [1/(V_{S1c} - f_2 V_S) - 1/V_{S1c}]\} \quad (12)$$

where $f_1 = \sigma'_v / (0.65 \sigma_v r_d)$ and $f_2 = (P_a / \sigma'_v)^{0.25}$. Assuming (1) the water table is located midway between the ground surface and the center of the most vulnerable layer and (2) the total unit weight of soil is 17.3 kN/m^3 above the water table and 18.9 kN/m^3 below the water table, then f_1 and f_2 can be approximated by:

$$f_1 \approx 1.1/r_d \quad (13)$$

and

$$f_2 \approx (7.3/z)^{0.25} \quad (14)$$

where z is depth to center of the most vulnerable layer in meters. For noncritical projects, this workshop suggests the following equations to estimate average values of r_d (Liao and Whitman):

$$r_d = 1.0 - 0.00765 z \quad \text{for } z \leq 9.15 \text{ m} \quad (15a)$$

$$r_d = 1.174 - 0.0267 z \quad \text{for } 9.15 \text{ m} < z \leq 23 \text{ m} \quad (15b)$$

Equations 12 through 15 provide a simple relationship between V_S and a_{max} that depends on depth. A relationship that depends on depth agrees with the analytical study by Stokoe et al. (1988b). For example, the critical values of V_S shown in Fig. 3c at a_{max} equal to $0.2 g$ and layer thickness of 3.0 m are about 110 m/s for a depth of 4.6 m and 170 m/s for a depth 12.2 m .

Liquefaction potential boundaries defined by Eqs. 12 through 15 are shown in Figs. 13, 14 and 15. Also shown are the case history data. Liquefaction behavior predicted by these boundaries is similar to behavior predicted by the boundaries based on V_{S1} and CRR. The three liquefaction case histories that lie slightly below the boundaries shown in Figs. 13a and 14c are the same three that lie slightly below the boundaries shown in Figs. 8a and 9c (Treasure Island UM06 and UM11, and Marina District School sites). Thus, the procedure based on V_S , a_{max} and depth is a good approximation to the recommended procedure based on V_{S1} and CRR.

The application of Eqs. 12 through 15 should be limited to sites with characteristics similar to the database (i.e., level ground, depth of most vulnerable layer less than 12 m , depth of water table $0.5\text{-}7.6 \text{ m}$, and uncemented soils of Holocene age).

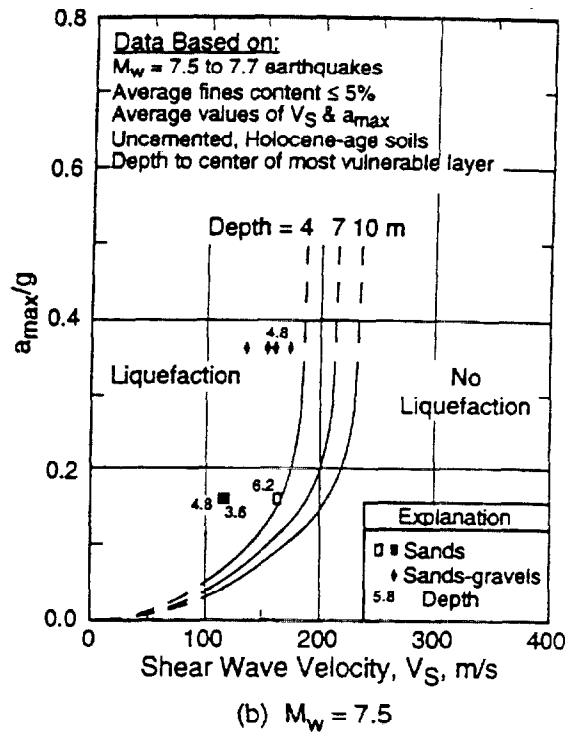
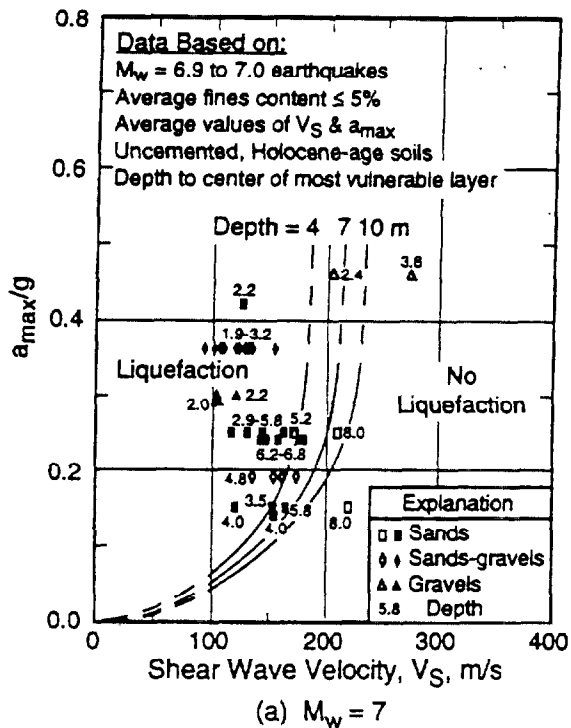


Fig. 13 - Comparison of Liquefaction Assessment Charts Based on V_S and Average a_{max} from Analysis for this Report with Case Histories of Uncemented Soils with Fines Content Less than or Equal to 5%.

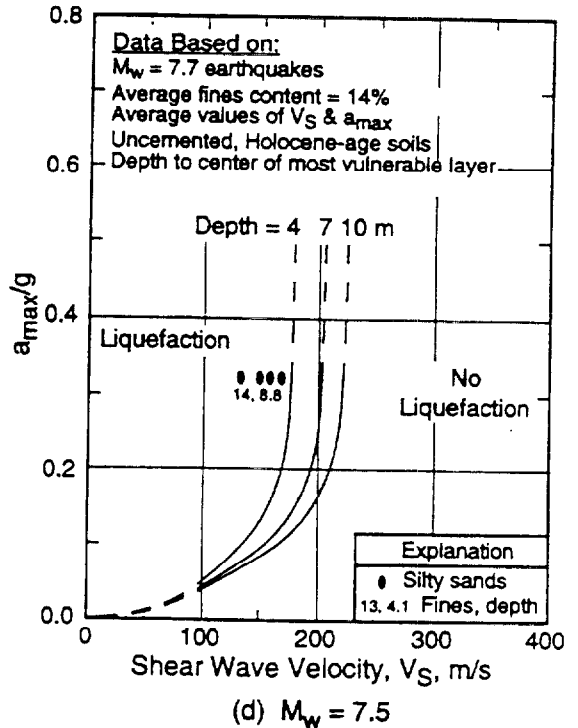
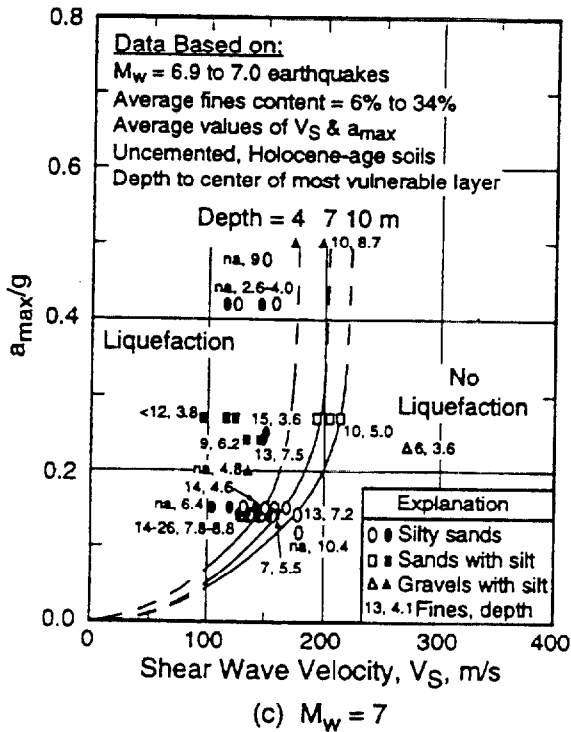
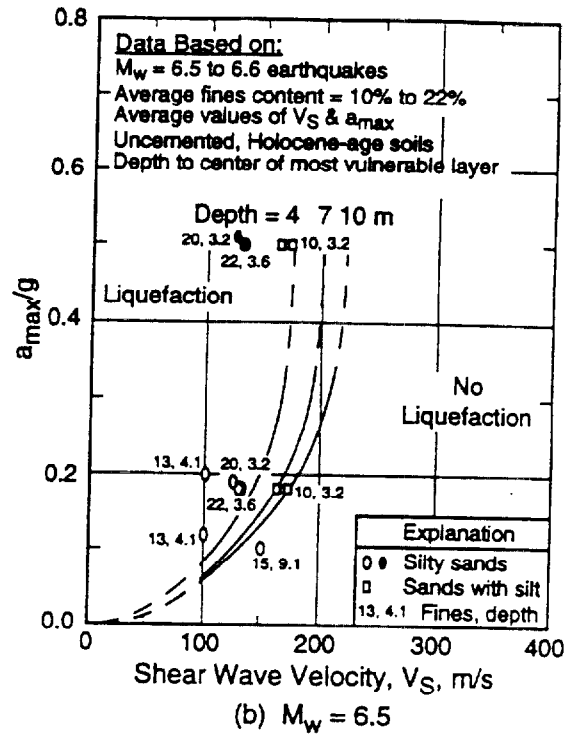
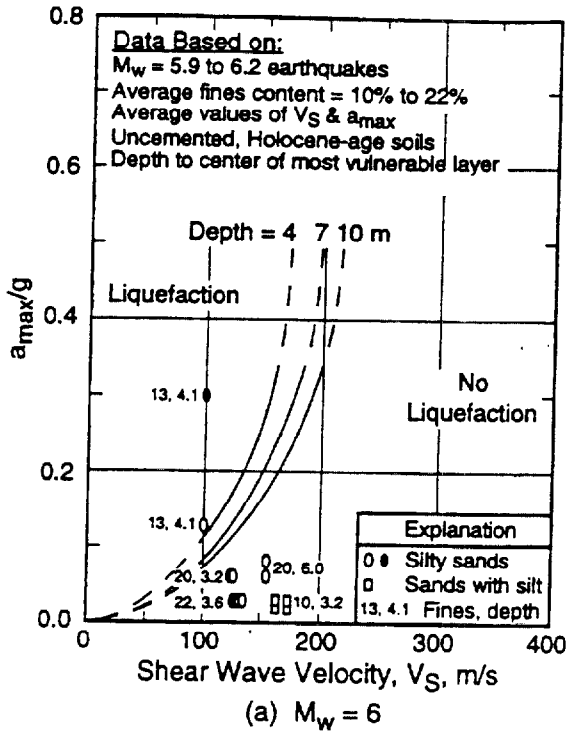
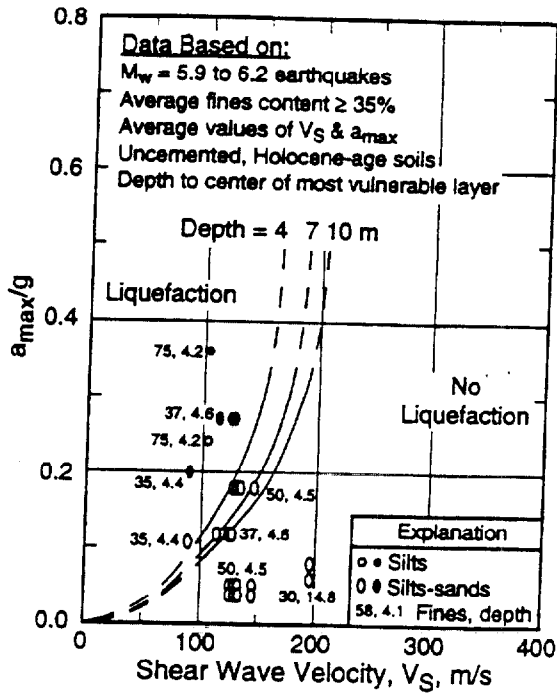
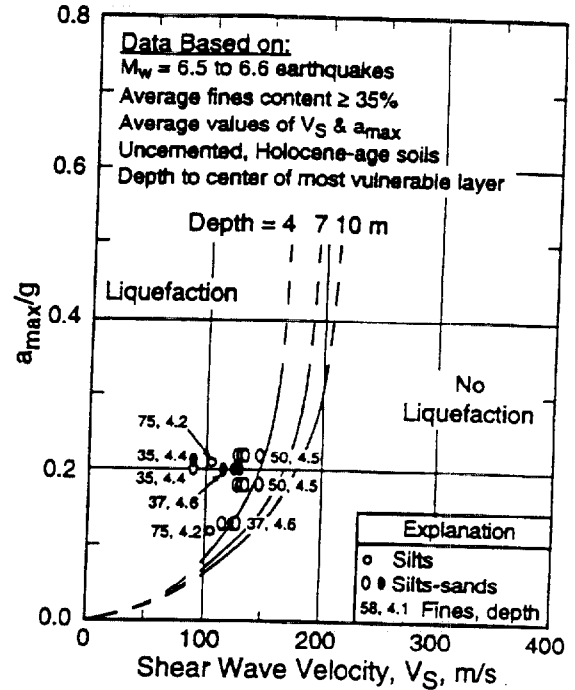


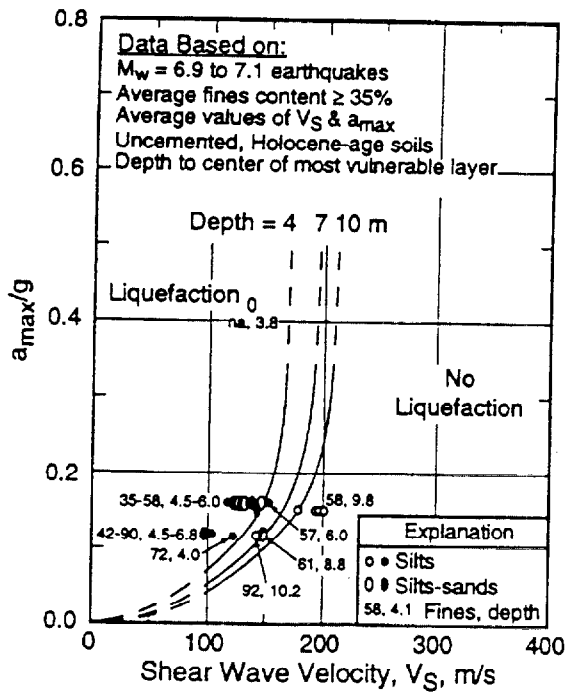
Fig. 14 - Comparison of Liquefaction Assessment Charts Based on V_S and Average a_{max} from Analysis for this Report with Case Histories of Uncemented Soils with Fines Content of 6% to 34%.



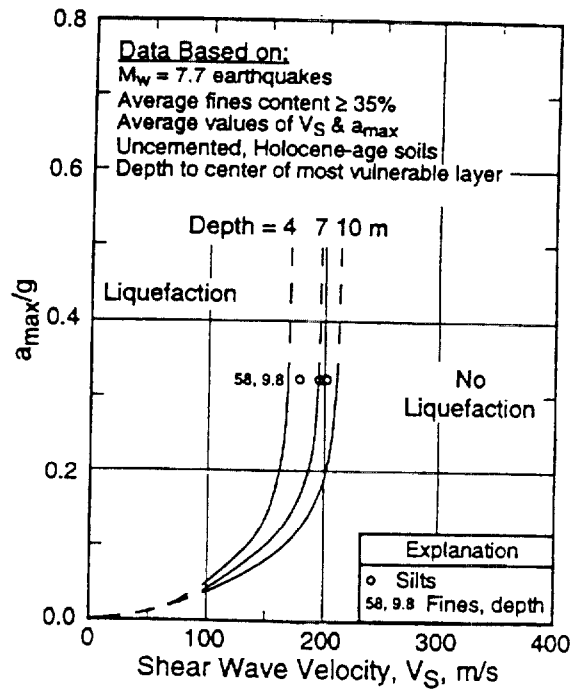
(a) $M_w = 6$



(b) $M_w = 6.5$



(c) $M_w = 7$



(d) $M_w = 7.5$

Fig. 15 - Comparison of Liquefaction Assessment Charts Based on V_S and Average a_{max} from Analysis for this Report with Case Histories of Uncemented Soils with Fines Content Greater than or Equal to 35%.

Conclusions and Recommendations

This report summarizes liquefaction and non-liquefaction case histories from 20 earthquakes and over 50 sites in soils ranging from sandy gravel with cobbles to profiles including silty clay layers. The data are limited to relatively level ground sites with the following characteristics: (1) depth of most vulnerable layer less than 12 m; (2) uncemented soils of Holocene age, with a few exceptions; and (3) depth of water table between 0.5 m and 7.6 m.

The compiled case histories are used to evaluate current liquefaction assessment procedures based on small-strain shear wave velocity. Most sites where surface manifestations of liquefaction were observed are correctly predicted by the current procedures. However, the boundaries by Stokoe et al. (1988b) are nonconservative at values of V_S less than about 180 m/s. The boundaries by Tokimatsu et al. (1991a) for earthquakes with greater than about 10 cycles of loading are nonconservative at values of V_{S1} greater than about 150 m/s. The boundary by Robertson et al. (1992) for earthquakes with magnitude of 7.5 is nonconservative at values of V_{S1} less than about 200 m/s. With few exceptions, the liquefaction case histories for earthquakes with magnitude of 7 are bounded by the relationships by Kayen et al. (1992) and Lodge (1994).

This workshop agreed that a careful review of the compiled case histories should be conducted. It was suggested that the recommended V_S -based procedure follow the general format of the CPT- and SPT-based procedures.

To develop the recommended liquefaction potential boundaries, the compiled case histories are separated into three categories: (1) sands and gravels with average fines content less than or equal to 5%; (2) sands and gravels with average fines content of 6% to 34%; and (3) sands and silts with average fines content greater than or equal to 35%. The data for two sites are not considered, since soils at these sites may be weakly cemented with carbonate. Representative values of V_{S1} for the most vulnerable layer and average values of a_{max} that would have occurred at the site in the absence of liquefaction are used. Values of V_{S1} are calculated using Eq. 4. Values of r_d are estimated using the relationship by Seed and Idriss (1971).

The recommended liquefaction potential boundaries are established by applying a modified relationship between V_{S1} and cyclic stress ratio for constant average cyclic shear strain suggested by Dobry (1996). The relationship by Dobry provides strong evidence for extending the boundaries to the origin. It is modified to become asymptotic to some limiting value of V_{S1} . This limit is caused by the tendency of dense granular soils to exhibit dilative behavior at large strains.

Figure 11 presents the recommended liquefaction potential boundaries for magnitude 7.5 earthquakes and uncemented Holocene-age soils. These boundaries are defined by Eq. 9 with $a = 0.03$, $b = 0.9$, and $V_{S1c} = 200$ m/s to 220 m/s depending on fines content.

Using scaling factors of 2.1, 1.6, 1.25 and 1.0 for earthquakes with magnitude of 6, 6.5, 7 and 7.5, respectively, provide boundaries that included more than 95% of the liquefaction case histories. These magnitude scaling factors lie within the range of scaling factors recommended by this workshop.

Caution should be exercised when applying the liquefaction potential boundaries to sites where conditions are different from the database. More work is needed to further validate and refine the values of V_{S1c} . Additional well-documented case histories of all types of soil that have and have not liquefied during earthquakes should be compiled, particularly from deeper deposits (depth > 8 m) and from denser soils ($V_S > 200$ m/s) shaken by stronger ground motions ($a_{max} > 0.4$ g), to further validate these boundaries.

Liquefaction potential boundaries based on V_S , a_{max} and depth defined by Eqs. 12 through 15 provide a good approximation to the recommended procedure based on V_{S1} and CRR. These simpler boundaries are suggested for initial site screening, and should be limited to sites with characteristics similar to the database.

Two limitations of using shear wave velocity are its high sensitivity to weak interparticle bonding, and the lack of a sample for identifying non-liquefiable clayey soils. Therefore, the preferred practice is to drill sufficient boreholes and take samples to verify or develop local correlations for soil types encountered, to identify non-liquefiable clay-rich soils, and to detect liquefiable weakly cemented soils. A combination of techniques may provide the most cost-effective approach for evaluating sites of large areal extent. In some cases, such as many landfills where borings are not permitted, evaluation based on shear wave velocity may be the only feasible approach.

Acknowledgments

The reporters thank the participants of this workshop for their constructive review, which greatly enhanced the quality of this report. Workshop participants included T. L. Youd (Chair), I. M. Idriss (Co-chair), I. Arango, G. Castro, J. T. Christian, R. Dobry, W. D. L. Finn, L. F. Harder, Jr., M. E. Hynes, K. Ishihara, J. P. Koester, S. S. C. Liao, W. F. Marcuson, III, G. R. Martin, J. K. Mitchell, Y. Moriwaki, M. S. Power, P. K. Robertson, and R. B. Seed. The review comments and encouragement of R. M. Chung are also greatly appreciated.

References

- Ambraseys, N. N. (1988). "Engineering Seismology," Earthquake Engineering and Structural Dynamics, Vol. 17, p. 1-105.
- Andrus, R. D., Stokoe, K. H., II, Bay, J. A., and Youd, T. L. (1992). "In Situ V_S of Gravelly Soils Which Liquefied," Proceedings, Tenth World Conference on Earthquake Engineering, held in Madrid, Spain, A.A. Balkema, Rotterdam, The Netherlands, pp. 1447-1452.
- Andrus, R. D. (1994). "In Situ Characterization of Gravelly Soils That Liquefied in the 1983 Borah Peak Earthquake," Ph.D. Dissertation, University of Texas at Austin, 533 p.
- Andrus, R. D., and Youd, T. L. (1987). "Subsurface Investigation of a Liquefaction-Induced Lateral Spread, Thousand Springs Valley, Idaho," Geotechnical Laboratory Miscellaneous Paper GL-87-8, U.S. Army Engineer Waterways Experiment Station, Vicksburg, MS, 131 p.
- Aouad, M. F. (1986). "Analytical Investigations of the Relationship between Shear Wave Velocity and the Liquefaction Potential of Sands," M.S. Report, Geotechnical Engineering Center, Department of Civil Engineering, University of Texas at Austin, 87 p.
- Arango, I. (1996). "Magnitude Scaling Factors for Soil Liquefaction Evaluations," Journal of Geotechnical Engineering, ASCE, Vol. 122, No. 11, pp. 929-936.
- Arulanandan, K., Yogachandran, C., Meegoda, N. J., Ying, L., and Zhouji, S. (1986). "Comparison of the SPT, CPT, SV and Electrical Methods of Evaluating Earthquake Induced Liquefaction Susceptibility in Ying Kou City During the Haicheng Earthquake," Proceedings, Use of In Situ Tests in Geotechnical Engineering, Geotechnical Special Publication No. 6, held in Blacksburg, Virginia, S. P. Clemence, Ed., ASCE, New York, NY, pp. 389-415.
- Barrow, B. L. (1983). "Field Investigation of Liquefaction Sites in Northern California," Geotechnical Engineering Thesis GT83-1, University of Texas at Austin, 213 p.
- Bennett, M. J. (1995). Personal communication to R. D. Andrus.
- Bennett, M. J., Youd, T. L., Harp, E. L., and Wieczorek, G. F. (1981). "Subsurface Investigation of Liquefaction, Imperial Valley Earthquake, California, October 15, 1979," Open-File Report 81-502, U.S. Geological Survey, 83 p.
- Bennett, M. J., McLaughlin, P. V., Sarmiento, J. S., and Youd, T. L. (1984). "Geotechnical Investigation of Liquefaction Sites, Imperial Valley, California," Open-File Report 84-252, U.S. Geological Survey, 103 p.

Bennett, M. J., and Tinsley, J. C. (1995). "Geotechnical Data from Surface and Subsurface Samples Outside of and within Liquefaction-Related Ground Failures Caused by the October 17, 1989, Loma Prieta Earthquake, Santa Cruz and Monterey Counties, California," Open-File Report 95-663, U.S. Geological Survey.

Bierschwale, J. G., and Stokoe, K. H., II (1984). "Analytical Evaluation of Liquefaction Potential of Sands Subjected to the 1981 Westmorland Earthquake," Geotechnical Engineering Report GR-84-15, University of Texas at Austin, 231 p.

Boulanger, R. W., Idriss, I. M., and Mejia, L. H. (1995). "Investigation and Evaluation of Liquefaction Related Ground Displacements at Moss Landing During the 1989 Loma Prieta Earthquake," Report No. UCD/CGM-95/02, University of California at Davis.

Boulanger, R. W., Mejia, L. H., and Idriss, I. M. (1997). "Liquefaction at Moss Landing During Loma Prieta Earthquake," Journal of Geotechnical and Geoenvironmental Engineering, ASCE, Vol. 123, No. 5, pp. 453-467.

Dobry, R. (1996). Personal communication to R. D. Andrus.

Dobry, R., Stokoe, K. H., II, Ladd, R. S., and Youd, T. L. (1981). "Liquefaction Susceptibility from S-Wave Velocity," Proc., In Situ Testing to Evaluate Liquefaction Susceptibility, ASCE National Convention, held in St. Louis, MO.

Dobry, R., Baziar, M. H., O'Rourke, T. D., Roth, B. L., and Youd, T. L. (1992). "Liquefaction and Ground Failure in the Imperial Valley, Southern California During the 1979, 1981 and 1987 Earthquakes," Case Studies of Liquefaction and Lifeline Performance During Past Earthquakes, Technical Report NCEER-92-0002, T. O'Rourke and M. Hamada, Eds., National Center for Earthquake Engineering Research, Buffalo, NY, Vol. 2.

Dobry, R., Ladd, R. S., Yokel, F. Y., Chung, R. M., and Powell, D. (1982). "Prediction of Pore Water Pressure Buildup and Liquefaction of Sands During Earthquakes by the Cyclic Strain Method," NBS Building Science Series 138, U.S. Department of Commerce, National Bureau of Standards, Gaithersburg, MD, 152 p.

EPRI (1992). Lotung Large-Scale Seismic Test Strong Motion Records, EPRI NP-7496L, Electric Power Research Institute, Palo Alto, California, Vols. 1-7.

Fuhriman, M. D. (1993). "Crosshole Seismic Tests at Two Northern California Sites Affected by the 1989 Loma Prieta Earthquake," M.S. Thesis, University of Texas at Austin, 516 p.

Geomatrix (1990). "Results of Field Exploration and Laboratory Testing Program for Perimeter Dike Stability Evaluation Naval Station Treasure Island San Francisco, California, Project No. 1539.05, Vol. 2.

Gibbs, J. F., Fumal, T. E., Boore, D. M., and Joyner, W. B. (1992). "Seismic Velocities and Geologic Logs from Borehole Measurements at Seven Strong-Motion Stations that Recorded the Loma Prieta Earthquake," Open-File Report 92-287, U.S. Geological Survey, 139 p.

Hardin, B. O., and Drnevich, V. P. (1972). "Shear Modulus and Damping in Soils: Design Equations and Curves," Journal of the Soil Mechanics and Foundation Division, ASCE, New York, NY, Vol. 98, SM7, pp. 667-692.

Hryciw, R. D. (1991). "Post Loma Prieta Earthquake CPT, DMT and Shear Wave Velocity Investigations of Liquefaction Sites in Santa Cruz and on Treasure Island," Final Report to the U.S. Geological Survey, Award No. 14-08-0001-G1865, University of Michigan, 68 p.

Hryciw, R. D., Rollins, K. M., Homolka, M., Shewbridge, S. E., and McHood, M. (1991). "Soil Amplification at Treasure Island During the Loma Prieta Earthquake," Proceedings, Second International Conference on Recent Advances in Geotechnical Earthquake Engineering and Soil Dynamics, held in St. Louis, Missouri, S. Prakash, Ed., University of Missouri-Rolla, Vol. II, pp. 1679-1685.

Idriss, I. M. (1996). Personal communication to T. L. Youd.

Ishihara, K., Shimizu, K., and Yamada, Y. (1981). "Pore Water Pressures Measured in Sand Deposits During an Earthquake," Soils and Foundations, Japanese Society of Soil Mechanics and Foundation Engineering, Vol. 21, No. 4, pp. 85-100.

Ishihara, K., Anazawa, Y., and Kuwano, J. (1987). "Pore Water Pressures and Ground Motions Monitored During the 1985 Chiba-Ibaragi Earthquake," Soils and Foundations, Japanese Society of Soil Mechanics and Foundation Engineering, Vol. 27, No. 3, pp. 13-30.

Ishihara, K., Muroi, T., and Towhata, I. (1989). "In-situ Pore Water Pressures and Ground Motions Monitored During the 1985 Chiba-Ibaragi Earthquake," Soils and Foundations, Japanese Society of Soil Mechanics and Foundation Engineering, Vol. 29, No. 4, pp. 75-90.

Kayen, R. E., Liu, H. -P., Fumal, T. E., Westerland, R. E., Warrick, R. E., Gibbs, J. F., and Lee, H. J. (1990). "Engineering and Seismic Properties of the Soil Column at Winfield Scott School, San Francisco," Effects of the Loma Prieta Earthquake on the Marina District San Francisco, California. Open-file Report 90-253, U.S. Geological Survey, pp. 112-129.

Kayen, R. E., Mitchell, J. K., Seed, R. B., Lodge, A., Nishio, S., and Coutinho, R. (1992). "Evaluation of SPT-, CPT-, and Shear Wave-Based Methods for Liquefaction Potential Assessment Using Loma Prieta Data," Proceedings, Fourth Japan-U.S. Workshop on Earthquake Resistant Design of Lifeline Facilities and Countermeasures for Soil Liquefaction. Technical Report NCEER-92-0019, held in Honolulu, Hawaii, M. Hamada and T. D. O'Rourke, Eds., National Center for Earthquake Engineering Research, Buffalo, NY, Vol. 1, pp. 177-204.

Kokusho, T., Sato, K., and Matsumoto, M. (1995a). "Nonlinear Seismic Amplification of Soil Ground During 1995 Hyogoken-Nanbu Earthquake," Proceedings, Fifth International Conference on Seismic Zonation, held in Nice, France, Presses Académiques, Vol. II, pp. 1603-1610.

Kokusho, T., Tanaka, Y., Kudo, K., and Kawai, T. (1995b). "Liquefaction Case Study of Volcanic Gravel Layer during 1993 Hokkaido-Nansei-Oki Earthquake," Proceedings, Third International Conference on Recent Advances in Geotechnical Earthquake Engineering and Soil Dynamics, held in St. Louis, Missouri, S. Prakash, Ed., University of Missouri-Rolla, Vol. I, pp. 235-242.

Kokusho, T., Yoshida, Y., and Tanaka, Y. (1995c). "Shear Wave Velocity in Gravelly Soils with Different Particle Gradings," Proceedings, Static and Dynamic Properties of Gravelly Soils, Geotechnical Special Publication No. 56, M. D. Evans and R. J. Fragaszy, Eds., ASCE, pp. 92-106.

Liao, S. S. C., and Whitman, R. V. (1986). "A Catalogue of Liquefaction and Non-liquefaction Occurrences During Earthquakes," Research Report, Dept. of Civil Engineering, M.I.T., Cambridge, MA.

Ladd, R. S. (1982). "Geotechnical Laboratory Testing Program for Study and Evaluation of Liquefaction Ground Failure Using Stress and Strain Approaches: Heber Road Site, October 15, 1979 Imperial Valley Earthquake," Woodward-Clyde Consultants, Wayne, New Jersey, February.

Lodge, A. L. (1994). "Shear Wave Velocity Measurements for Subsurface Characterization," Ph.D. Dissertation, University of California at Berkeley.

Mitchell, J. K., Lodge, A. L., Coutinho, R. Q., Kayen, R. E., Seed, R. B., Nishio, S., and Stokoe, K. H., II (1994). "Insitu Test Results from Four Loma Prieta Earthquake Liquefaction Sites: SPT, CPT, DMT, and Shear Wave Velocity," Report No. UCB/EERC-94/04, Earthquake Engineering Research Center, University of California at Berkeley, 171 p.

Ohta, Y., and Goto, N. (1976). "Estimation of S-Wave Velocity in Terms of Characteristic Indices of Soil," Butsuri-Tanko (Geophysical Exploration), Vol. 24, No. 4, pp. 34-41 (in Japanese).

Redpath, B. B. (1991). "Seismic Velocity Logging in the San Francisco Bay Area," Report to the Electric Power Research Institute, Palo Alto, California, 34 p.

Robertson, P. K., Woeller, D. J., and Finn, W. D. L. (1992). "Seismic Cone Penetration Test for Evaluating Liquefaction Potential Under Cyclic Loading," Canadian Geotechnical Journal, Ottawa, Canada, Vol. 29, pp. 686-695.

Rollins, K. M., McHood, M. D., Hryciw, R. D., Homolka, M., and Shewbridge, S. E. (1994). "Ground Response on Treasure Island," The Loma Prieta, California, Earthquake of October 17, 1989--Strong Ground Motion, U.S. Geological Survey Professional Paper 1551-A, R. D. Borcherdt, Ed., United States Government Printing Office, Washington, pp. A109-A121.

Roy, D., Campanella, R. G., Byrne, P. M., and Hughes, J. M. O. (1996). "Strain Level and Uncertainty of Liquefaction Related Index Tests," Proceedings, Uncertainty in the Geologic Environment: From Theory to Practice, Geotechnical Special Publication No. 58, held in Madison, Wisconsin, C. D. Shackelford, P. P. Nelson, and M. J. S. Roth, Eds., ASCE, Vol. 2, pp. 1149-1162.

Sato, K., Kokusho, T., Matsumoto, M., and Yamada, E. (1996). "Nonlinear Seismic Response and Soil Property During Strong Motion," Soils and Foundations, Special Issue on the 1995 Hyogoken-Nambu Earthquake, Japanese Geotechnical Society, January, pp. 41-52.

Schnabel, P. B., Lysmer, J., and Seed, H. B. (1972). "SHAKE: A Computer Program for Earthquake Response Analysis of Horizontally Layered Sites," Earthquake Engineering Research Center Report No. UCB/EERC-72-12, University of California, Berkeley.

Seed, H. B. (1979). "Soil Liquefaction and Cyclic Mobility Evaluation for Level Ground During Earthquakes," Journal of the Geotechnical Engineering Division, ASCE, New York, NY, Vol. 105, GT2, pp. 201-255.

Seed, H. B., and Idriss, I. M. (1971). "Simplified Procedure for Evaluating Soil Liquefaction Potential," Journal of the Soil Mechanics and Foundation Division, ASCE, New York, NY, Vol. 97, SM9, pp. 1249-1273.

Seed, H. B., and Idriss, I. M. (1982). Ground Motions and Soil Liquefaction During Earthquakes, monograph series, Earthquake Engineering Research Institute, Berkeley, California, 134 p.

Seed, H. B., Idriss, I. M., and Arango, I. (1983). "Evaluation of Liquefaction Potential Using Field Performance Data," Journal of Geotechnical Engineering Division, ASCE, New York, NY, Vol. 109, No. 3, pp. 458-482.

Seed, H. B., Tokimatsu, K., Harder, L. F., and Chung, R. M. (1985). "Influence of SPT Procedures in Soil Liquefaction Resistance Evaluations," Journal of Geotechnical Engineering Division, ASCE, Vol. 111, No. 12, pp. 1425-1445.

Shen, C. K., Li, X. S., and Wang, Z. (1991). "Pore Pressure Response During 1986 Lotung Earthquakes," Proceedings, Second International Conference on Recent Advances in Geotechnical Earthquake Engineering and Soil Dynamics, held in St. Louis, Missouri, S. Prakash, Ed., University of Missouri-Rolla, Rolla, Mo., Vol. I, pp. 557-563.

Shibata, T., Oka, F., and Ozawa, Y. (1996). "Characteristics of Ground Deformation Due to Liquefaction," Soils and Foundations, Special Issue on the 1995 Hyogoken-Nambu Earthquake, Japanese Geotechnical Society, January, pp. 65-79.

Stokoe, K. H., II, Andrus, R. D., Bay, J. A., Fuhrman, M. D., Lee, N. J., and Yang, Y. (1992). "SASW and Crosshole Seismic Test Results from Sites that Did and Did not Liquefy During the 1989 Loma Prieta, California Earthquake," Geotechnical Engineering Center, Department of Civil Engineering, University of Texas at Austin.

Stokoe, K. H., II, and Nazarian, S. (1985). "Use of Rayleigh Waves in Liquefaction Studies," Proceedings, Measurement and Use of Shear Wave Velocity for Evaluating Dynamic Soil Properties, held in Denver, Colorado, R. D. Woods, Ed., ASCE, New York, NY, pp. 1-17.

Stokoe, K. H., II, Andrus, R. D., Rix, G. J., Sanchez-Salinerio, I., Sheu, J. C., and Mok, Y. J. (1988a). "Field Investigation of Gravelly Soils Which Did and Did Not Liquefy During the 1983 Borah Peak, Idaho, Earthquake," Geotechnical Engineering Center Report GR 87-1, University of Texas at Austin, 206 p.

Stokoe, K. H., II, Roesset, J. M., Bierschwale, J. G., and Aouad, M. (1988b). "Liquefaction Potential of Sands from Shear Wave Velocity," Proceedings, Ninth World Conference on Earthquake Engineering, held in Tokyo, Japan, Vol. III, pp. 213-218.

Sugito, M., Sekiguchi, K., Oka, F., and Yashima, A. (1996). "Analysis of Borehole Array Records from the South Hyogo Earthquake of Jan. 17, 1995," Proceedings of the International Workshop on Site Response Subjected to Strong Earthquake Motions, held in Yokosuka, Japan on January 15-17, Port and Harbor Research Institute, Yokosuka, Japan, Vol. 2, pp. 343-357.

Sykora, D. W., and Stokoe, K. H., (1982), "Seismic Investigation of Three Heber Road Sites After the Oct. 15, 1979 Imperial Valley Earthquake," Geotechnical Engineering Report GR82-24, University of Texas at Austin.

Tokimatsu, K., Kuwayama, S., and Tamura, S. (1991a). "Liquefaction Potential Evaluation Based on Rayleigh Wave Investigation and Its Comparison with Field Behavior," Proceedings, Second International Conference on Recent Advances in Geotechnical Earthquake Engineering and Soil Dynamics, held in St. Louis, Missouri, S. Prakash, Ed., University of Missouri-Rolla, Rolla, Mo., Vol. I, pp. 357-364.

Tokimatsu, K., Kuwayama, S., Abe, A., Nomura, S., and Tamura, S. (1991b). "Considerations to Damage Patterns in the Marina District During Loma Prieta Earthquake Based on Rayleigh Wave Investigation," Proceedings, Second International Conference on Recent Advances in Geotechnical Earthquake Engineering and Soil Dynamics, held in St. Louis, Missouri, S. Prakash, Ed., University of Missouri-Rolla, Vol. II, pp. 1649-1654.

Turner, E. and Stokoe, K. H., II (1992). "Static and Dynamic Properties of Clayey Soils Subjected to the 1979 Imperial Valley Earthquake," Geotechnical Engineering Report GR82-26, University of Texas at Austin, 208 p.

Youd, T. L., and Noble, S. K. (in press). "Magnitude Scaling Factors," Proceedings, NCEER Workshop on Evaluation of Liquefaction Resistance, held in Salt Lake City, Utah, T. L. Youd and I. M. Idriss, Eds., National Center for Earthquake Engineering Research, Buffalo, NY.

Youd, T. L., and Bennett, M. J. (1983). "Liquefaction Sites, Imperial Valley, California," Journal of Geotechnical Engineering Division, ASCE, Vol. 109, No. 3, pp. 440-457.

Youd, T. L., and Hoose, S. N. (1978). "Historic Ground Failures in Northern California Triggered by Earthquakes," U.S. Geological Survey Professional Paper 993, 177 p.